ACS Catalysis

pubs.acs.org/acscatalysis

Review

Critical Review of Catalysis for Ethylene Oxychlorination

Hongfei Ma,[§] Yalan Wang,[§] Yanying Qi,[§] Kumar R. Rout,* and De Chen*

Cite This: *ACS Catal.* 2020, 10, 9299−9319

Read Online

ACCESS | Metrics & More | Article Recommendations

ABSTRACT: Ethylene oxychlorination is the key technology in vinyl chloride (VCM, the monomer of PVC, polyvinyl chloride) production to close the chlorine loop by consuming the HCl released from the former cracking step. Due to the high demand for PVC, this leads to ethylene oxychlorination being one of the most important processes in the industry. This Review covers an in-depth analysis of the dynamic nature of active sites for the main and side reactions involved in ethylene oxychlorination, featuring the findings and viewpoints from the dynamic kinetics study and analysis under industrial operating conditions. A unified picture of the mechanism of the surface reactions, and the effect of supports and promoters, has been presented based on the decoupled redox-cycle experiments, which leads to a significantly better understanding of the mechanism and provides valuable guidelines for effective catalyst design. Operando techniques and kinetic tools of the rate-diagram, as well as their application to the study of the redox-cycle in ethylene oxychlorination and kinetic models on both the main product and byproduct, are also reviewed. Perspectives on challenges and new process development and future research focus for better study of the VCM production chemistry are also proposed.

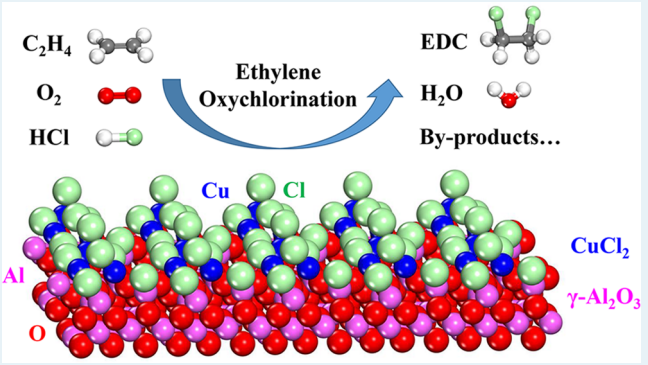

KEYWORDS: *$CuCl_2/\gamma\text{-}Al_2O_3$, active site, ethylene oxychlorination, kinetics, reaction mechanisms*

1. INTRODUCTION

Polyvinyl chloride (PVC) is one of the most commonly used plastic materials that has a wide range of applications, such as in households and construction, electronics, pharmaceutical, and automotive industries.[1] It is produced through the polymerization of its monomer vinyl chloride (VCM).[2] The high demand and global increase in PVC led to VCM being one of the most precious chemicals. In 2018, the global VCM production capacity was approximately 49 million metric tons, which is expected to increase to around 52.9 million metric tons in 2023.[3] There are two main routes by which VCM is produced industrially. One is direct hydrochlorination of acetylene;[4,5] another is cracking of ethylene dichloride (EDC) provided by direct chlorination[6−9] and/or oxychlorination of ethylene.[10−12] The combination of direct chlorination, ethylene oxychlorination, and EDC cracking is named as the "balanced VCM process" (Figure 1).[13] In addition to the above two routes, ethane oxychlorination is another promising route for VCM production due to the economic advantage of feedstock.[1,14−18] However, despite the efforts of several decades, ethane-based technology is still under exploration and has not been commercialized yet. Other technologies are developed either based on feedstocks or catalysts of the three routes. To date, among these different technologies, the ethylene route is predominant and attracts much attention, based on that more than 90% of the VCM production plants worldwide are using the balanced VCM process.[19]

The oxychlorination of lower hydrocarbons (C_1-C_4) was an active research topic for both academic research and industrial applications, and the topic was reviewed by two groups in the 1980s including thermodynamics, catalysts, kinetics, mechanisms, as well as the technology of the process.[16,20] Recently Lin et al.[1] have reviewed different processes for halogen-mediated conversion of hydrocarbons to commodities, among which the PVC (or VCM) production is one of the important topics. However, despite the excellent reviews, a critical review for ethylene oxychlorination which has played such a vital role in VCM production is still missing, which is essential for gaining a better understanding of the reaction and developing more efficient catalysts.

Herein, we will critically review the progress of the catalyst developments toward better activity, selectivity, and stability for ethylene oxychlorination with a focus on the reaction

Received: April 15, 2020
Revised: July 16, 2020
Published: July 20, 2020

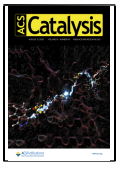

https://dx.doi.org/10.1021/acscatal.0c01698
ACS Catal. 2020, 10, 9299−9319

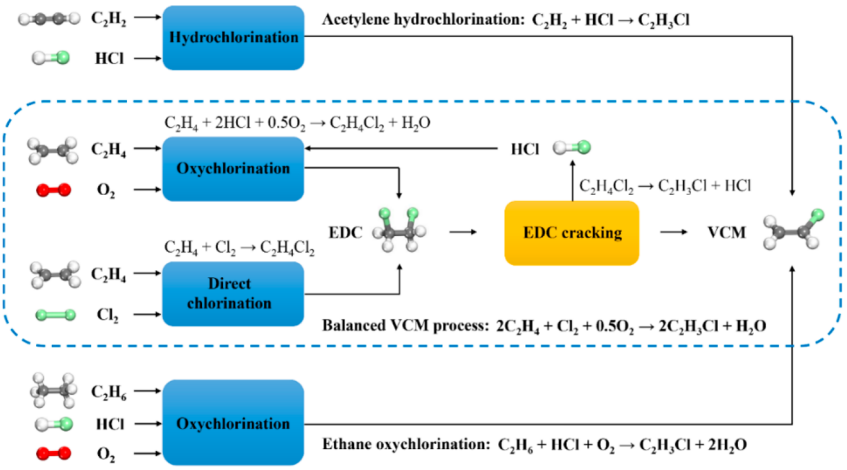

Figure 1. Production of VCM by three different routes: acetylene hydrochlorination, ethylene direct chlorination/oxychlorination, and ethane oxychlorination.

mechanism, site requirement, and catalyst design. The goal will be approached by a detailed analysis of the effects of metal chloride identities, supports, and promoters on catalytic performances of most common $CuCl_2$-based catalysts including reactions leading to both main and byproducts formation. Particular attention will be paid to the effect of catalyst properties on the individual reaction steps in a catalytic cycle including reduction of $CuCl_2$ by ethylene, oxidation of CuCl by oxygen, and hydrochlorination of Cu_2OCl_2 by HCl and their effect on the dynamic evolution of active sites in the redox cycle, which is the key toward effective catalysts.

2. ETHYLENE OXYCHLORINATION CATALYSTS

As early as 1966, Todo, Kurita, and Hagiwara already discovered metal chlorides active for ethylene oxychlorination.[21] The catalytic activity of these catalysts followed the order of $CrCl_3 > CuCl_2 > FeCl_3 > MnCl_2 > NiCl_2$. However, $CuCl_2$ was found to show higher selectivity for EDC formation than $CrCl_3$. Hall et al. have measured the adsorption heat of ethylene at low temperatures (<150 °C) on a series of unsupported transition metal chlorides with varied d-electrons by a gas-adsorption chromatography method in 1984.[14] The ethylene adsorption heat follows an order of $CuCl_2 > NiCl_2 > CrCl_3 > FeCl_2 > CoCl_2 > VCl_3 > MgCl_2 > CrCl_2 > MnCl_2 >$ CuCl. It was found that ethylene physically adsorbed on $CrCl_2$, $MnCl_2$, and CuCl had no activity. The transition metal chlorides can be classified into two groups, namely divalent and trivalent chlorides. The chemisorption of ethylene seemed to be occurring on divalent $CuCl_2$ and $NiCl_2$. $CuCl_2$ exhibited high activity of reduction and high selectivity for EDC, while there was no reaction between ethylene and $NiCl_2$. Intermediate adsorption of ethylene was observed on VCl_3, $CrCl_3$, $FeCl_2$, and $CoCl_2$. VCl_3 displayed activity to VCM but was prone to deactivation due to high volatility at high temperatures. VCM and EDC were formed on $CrCl_3$ at 523 K, but an undesired hydrocarbon polymer (nonchlorine-containing) was also produced. Besides the above transition metal chlorides, some noble metal chlorides were also tried as catalysts for ethylene oxychlorination with high selectivity to VCM, such as $PdCl_2$, $PtCl_2$, $RhCl_3$, and $RuCl_3$.[16,20] The catalyst activity for formation of VCM followed the order $PdCl_2 > RhCl_3 > PtCl_2 > RuCl_3$. The highest selectivity to VCM was obtained over Pd-containing catalysts. However, the limited activity was a drawback of these catalysts. To summarize, no metal chlorides can compete with $CuCl_2$ in the selective formation of EDC.

In addition to the above studies, more efforts have been made to explore efficient catalysts for ethylene oxychlorination. A large number of catalysts have been developed over the past half-century, and their catalytic performances are summarized in Table 1. Among various catalysts, copper chloride ($CuCl_2$) was identified as a superior catalyst for ethylene oxychlorination owing to its high activity and selectivity.[14,22] Why is this so? It might be roughly explained by an interesting hypothesis presented by Allen,[23] namely the smaller the standard free energy changes related to individual steps of the Deacon reaction, the better the Deacon catalyst, such as $CuCl_2$ in eqs 1 and 2:

$$2CuCl_2 + 1/2O_2(g) \rightarrow CuO{\cdot}CuCl_2(s) + Cl_2(g)$$
$$\Delta G_{298-900K} = +57 \text{ to } +6 \text{ kJ/mol} \quad (1)$$

$$CuO{\cdot}CuCl_2(s) + 2HCl \rightarrow 2CuCl_2(s) + H_2O$$
$$\Delta G_{298-900K} = -84.4 \text{ to } -5.4 \text{ kJ/mol} \quad (2)$$

$$2CuCl_2(s) \rightleftharpoons 2CuCl(s) + Cl_2(g)$$
$$\Delta G_{298-900K} = +142 \text{ to } 60 \text{ kJ/mol} \quad (3)$$

The calculated standard free energies for each Deacon step were in the following order by replacing Cu with other divalent metals.[23,24]

$$Mg < Cu < Sn(II) < Ni < Zn < Rh < Fe(II) < V(II) < Mn < Co < Pd < Cd < Hg < Pb < Ca < Sr < Ba$$

It indicates that among all investigated metals, Mg is the only one more favorable than Cu. However, Mg cannot undergo redox reactions (eq 3) because of existing only in the +2-oxidation state. Like Mg, most lanthanides are not redox-active although they exhibit also low Gibbs free energy for reaction eqs 1 and 2. This might explain why Mg and rare earth are not superior catalysts but can be used as promoters for ethylene oxychlorination in combination with cupric chloride. Since the ethylene chlorination by reduction step is not considered in the above analysis, a direct prediction of

https://dx.doi.org/10.1021/acscatal.0c01698
ACS Catal. 2020, 10, 9299−9319

Table 1. Ethylene Oxychlorination Catalysts

year	catalysts	T (K)	C_2H_4/O_2/HCl (molar)	C_2H_4 conversion (%)	EDC selectivity (%)	VCM selectivity (%)	EtCl selectivity (%)	main conclusions	ref
1969	iron oxide-containing catalyst	773	1:2.5:2.5	50.7	9.7	61.8		Deuterium labeling experiments support a mechanism involving EDC as the VCM precursor.	27
1971	$CuCl_2/\gamma$-Al_2O_3	553	1:3:2	98.8	97.0		0.2	excellent catalytic performance	26
1972	$PdCuNaCl_x$		1:1:3					$PdCuNaCl_x$, $PdFeNaCl_x$, and $PtFeNaCl_x$ exhibited better performance than others did.	25
	$PdFeCl_x$	547		97.2	81.5	8.1	0.1		
	$PdFeNaCl_x$	589		41.5	1.7	44.9	8.6		
	$PdFeKCl_x$	561		88.1	25.2	60.2	3.1		
	$RuFeNaCl_x$	589		84.9	6.0	57.0	0.9	For $PdFeNaCl_x$, replacing Fe by Cr, Mn, Co, Ni, Ag, W, Pt, and Ce resulted in very low ethylene conversion (<7%); replacing Na by Mg, Ca, Ba, Pb, Bi, Li, Zn, Ag, and K led to both lower ethylene conversion and VCM selectivity.	
	$IrFeNaCl_x$	616		81.7	60.4	11.5	1.0		
	$RhFeNaCl_x$	616		61.7	35.6	37.3	3.9		
	$PtFeNaCl_x$	589		77.2	74.7	20.6	1.8		
	support: Al_2O_3	561		100.0	80.8	14.1	1.0		
1978	$RhFeZnLiCl_x/\alpha$-Al_2O_3	623	1:2:2	29−46	17−53	42−77		Rh, Fe, and Zn are essential components, while Li is an optional component to extend catalyst life.	28
1991	fly ash	773	1:6.4:3.5	61	0.9	11.4		low EDC and VCM selectivity	29
2005	LaOCl	672	3.6:1:2	23.7	11.3	75.3	3.5	LaOCl exhibited better performance than other rare-earth catalysts and catalysts containing two rare-earth materials, as well as catalysts containing rare-earth materials with other additives.	32
	NdOCl	676	4.2:1:2.3	13.2	2.9	74.4	6.9		
	PrOCl	674	3.7:1:2	22.8	6.1	74.2	4.4		
	SmOCl	673	3.6:1:2	14.7	2.9	61.0	10.6		
	$HoCl_3$	673	3.6:1:2	12.7	14.5	33.3	16.8		
	$ErCl_3$	673	3.6:1:2	15.4	17.5	44.0	12.8		
	$YbCl_3$	673	4.2:1:2.3	3.3	8.8	6.1	37.0		
	YCl_3	672	3.6:1:2	13.8	18.8	35.0	16.5		
	$LaCl_3$−$NdCl_3$	674	3.7:1:2	16.8	9.7	75.8	4.1		
	$LaCl_3$−$SmCl_3$	674	3.6:1:2	11.3	7.5	51.0	11.8		
	$LaCl_3$−YCl_3	673	3.6:1:2	12.5	12.4	51.4	8.9		
	$LaCl_1$−$HoCl_3$	672	3.6:1:2	12.4	14.5	28.9	17.0		
	$LaCl_3$−$HoCl_3$	673	3.6:1:2	9.2	20.6	11.1	23.8		
	$LaCl_3$−CeO_2	673	3.7:1:2	18.2	11.5	64.5	5.0		
2016	EuOCl	673	1:1:1.6	10	25	75	0	Except for CeO_2 and EuOCl, other lanthanide (La, Pr, Nd, Sm, Gd, Tb, Dy, Ho, Er) catalysts mainly led to undesired CO_x production. EuOCl exhibited the best EDC/VCM selectivity; CeO_2 showed the highest activity; coupling them led to a better VCM yield.	33
	CeO_2	673		26	76	15	0		
	EuOCl-CeO_2	673		22	5	95	0		
2016	$CuKLaCl_x/Al_2O_3$	473	1:1:1.6	12	100	0	0	$CuKLaCl_x/Al_2O_3$- and CeO_2-based catalysts displayed high EDC/VCM selectivity; IrO_2 and RuO_2 mainly led to undesired CO_x production.	30
	IrO_2	673		11	0	0	0		
	RuO_2	673		9	7	3	0		
	CeO_2	623		13	92	6	0		
	CeO_2−ZrO_2	673		60	45	43	0		
2017	RuO_2	573	2:1:2	7	55	15	0	Performance needs to be improved.	31
2018	$CeCl_3$	723	1:1:1.6	58	10	40	0	For $CeCl_3$, CeOCl, and CeO_2, the catalyst bulk phase is CeO_2, with CeOCl contained in the surface.	34
	CeOCl	723		50	8	25	0		

https://dx.doi.org/10.1021/acscatal.0c01698
ACS Catal. 2020, 10, 9299−9319

Table 1. continued

year	catalysts	T (K)	$C_2H_4/O_2/HCl$ (molar)	C_2H_4 conversion (%)	EDC selectivity (%)	VCM selectivity (%)	EtCl selectivity (%)	main conclusions	ref
	CeO_2	723		33	15	25	0		

oxychlorination catalysts cannot be achieved only based on Allen's model. Therefore, more research was performed on this process.

In 1972, Dugan et al. conducted ethylene oxychlorination by using the $PdFeNaCl_x/Al_2O_3$ catalyst and a series of its derivative catalysts, with $PdCuNaCl_x/Al_2O_3$ as a benchmark (Table 1).[25] Among all studied catalysts, $PdFeNaCl_x/Al_2O_3$ and $PtFeNaCl_x/Al_2O_3$ exhibited comparable performance to $PdCuNaCl_x/Al_2O_3$, better than the others did. The superior performance of the two catalysts was attributed to the promotion effect of Na. It can be seen that without Na, the catalytic performance of the $PdFeCl_x/Al_2O_3$ catalyst was greatly reduced and cannot compete with that of the $CuCl_2/\gamma$-Al_2O_3 catalyst.[26] Besides, the iron oxide-containing catalysts,[27] the $RhFeZnLiCl_x/\alpha$-Al_2O_3 catalyst,[28] fly ash,[29] IrO_2,[30] and RuO_2[30,31] have been also demonstrated active for ethylene oxychlorination. However, both lower activity and EDC/VCM selectivity were observed over these catalysts than the $CuCl_2/\gamma$-Al_2O_3 catalyst.[26] Recently, the use of rare-earth catalysts for ethylene oxychlorination to VCM has stimulated great interest.[30,32−34] In 2005, Jones et al. investigated ethylene oxychlorination over various rare-earth (La, Nd, Pr, Sm, Ho, Er, Yb, and Y) catalysts.[32] Among them, LaOCl exhibited better performance than other rare-earth catalysts and catalysts containing two rare-earth materials, as well as catalysts containing rare-earth materials with other additives. The study of Scharfe et al. in 2016 illustrated that toward researched lanthanide (Eu, Ce, La, Pr, Nd, Sm, Gd, Tb, Dy, Ho, Er) catalysts, EuOCl displayed the best EDC/VCM selectivity, and CeO_2 showed the highest activity; coupling them (EuOCl-CeO_2) led to a better VCM yield.[33] Inspired by the acceptable activity of CeO_2, another study of Scharfe et al. attempted to improve the CeO_2 performance by coupling CeO_2 with ZrO_2. The newly prepared CeO_2−ZrO_2 catalyst conducted stable ethylene conversions (60%) and high selectivity to EDC/VCM (45% for EDC, 43% for VCM).[30] The lanthanide catalysts have poor activity at low temperatures and were only active at high temperatures typically larger than 673 K. These catalysts have relatively high selectivity of VCM and can be considered as the promising ways for process intensification to integrate the oxychlorination and dehydrochlorination into one single step. Continuous efforts should be focused on this active area to make the VCM yield higher and cost-effective in the future.

Currently, $CuCl_2$-based catalysts are still the most used industrial catalysts and show better catalytic performance for EDC production. Since the first industrial ethylene oxychlorination plant was built by Dow in the USA in 1955, the $CuCl_2$-based catalysts have been used as the industrial catalysts. There has been a challenge of the high volatility of cuprous chloride, caused by a loss of the active component and aggregation on both fixed-bed and fluidized-bed catalysts. It has drawn great academic and industrial interests to gain a better understanding of the surface reaction mechanism, dynamics in redox cycle, active sites, effects of support, and promoters, to improve the catalytic performance in terms of activity, selectivity, and especially the stability through improving the formulation of the oxychlorination catalysts. Therefore, in the following part, we will focus on a review of $CuCl_2$-based catalysts for ethylene oxychlorination to EDC production.

https://dx.doi.org/10.1021/acscatal.0c01698
ACS Catal. 2020, 10, 9299−9319

3. Cu-BASED CATALYSTS FOR ETHYLENE OXYCHLORINATION

3.1. Cu Species in $CuCl_2/\gamma$-Al_2O_3. $CuCl_2/\gamma$-Al_2O_3-based catalysts are widely used industrial catalysts, and considerable research has been employed to exploit the nature of active sites.[35−40] Generally, the catalysts were prepared by the incipient wetness impregnation method; after impregnation, the samples were dried at 120 °C under the dry airflow for 12 h. In the catalysts, six Cu species, namely paratacamite, copper alumina surface species, cupric chloride ($CuCl_2$), $CuCl_2$ with the vacancy, Cu oxide chloride (Cu_2OCl_2), and cuprous chloride (CuCl), have been observed.

Paratacamite ($Cu_2(OH)_3Cl$). The $CuCl_2$-based catalysts are typically prepared by impregnation. The catalyst preparation and pretreatment were studied by Density Functional Theory (DFT) calculations.[39] It is found that the adsorption of Cu^{2+} and Cl^- is structure sensitive and also significantly sensitive to hydration and dehydration. Both Cu^{2+} and Cl^- adsorb exclusively on the (110) and (100) surfaces of γ-alumina but not on the (111) surface. On the (100) surface, both chloride ions bind to the copper. On the (110) surface, only one chloride binds to the copper, and the other binds to the alumina surface. The predicted results were validated by experiments using temperature-programmed desorption (TPD) and temperature-programmed reduction (TPR). The results reveal that catalyst preparation and properties are structure sensitive to the alumina. The γ-Al_2O_3 is an inert material to provide a large surface area to deposit $CuCl_2$. The morphology and particle size of the γ-Al_2O_3 should be addressed. Lamberti and co-workers characterized the fresh Al_2O_3-supported $CuCl_2$ for ethylene oxychlorination, by ultraviolet−visible and near-infrared spectroscopy (UV−vis-NIR), a solubility test, electron paramagnetic resonance (EPR), extended X-ray absorption fine structure (EXAFS), and X-ray diffraction (XRD) techniques in a wide range (0.25−9.0 wt %) of Cu loading.[37,38] It is found that three different copper species are present: a highly dispersed copper chloride phase, a Cu-aluminate phase, and an aggregated paratacamite phase.[37,38] Both DFT calculation and experimental results revealed that after impregnation, surface $CuCl_2 \cdot 2H_2O$ formed during drying and gradually pyrolyzed with further heating to form paratacamite. The HCl released during the hydrolysis reacts with alumina forming a >Al−Cl species (eq 4).

$$2CuCl_2 + 3(>Al{-}OH) \rightarrow Cu_2(OH)_3 + 3(>Al{-}Cl) \quad (4)$$

The paratacamite phase is formed due to being stored in the atmosphere. Under the treatment at the reaction temperature in the presence of HCl, the paratacamite transfers into copper chloride, and the catalyst can be completely activated.

Copper Alumina Surface Species. The copper ions occupy octahedral vacancies of the alumina surface in the inactive surface copper aluminate, which forms at low loadings. The $CuCl_2$ appeared as a highly asymmetric structure, and it is stable against washing treatment with solvent.[41,42] These sites are inactive for the oxychlorination reaction. The amount of surface Cu alumina species can be reduced by adding promoters.

Cupric Chloride ($CuCl_2$). The amorphous $CuCl_2$, formed at high loadings, is the active phase for the oxychlorination of ethylene. The properties of the amorphous $CuCl_2$ are briefly summarized here:[38] (i) it shows spherical symmetry evidenced by a very broad EPR signal; (ii) it is soluble; (iii) it starts to appear when the alumina surface is saturated to form surface copper aluminate; (iv) it is characterized by a very intense d−d band at about 13,000 cm^{-1} and an additional charge transfer band in the 28,000 to 31,000 cm^{-1} range in UV−vis spectroscopy, and d−d band intensity is proportional to the concentration of $CuCl_2$; (v) it is not stable upon both thermal and vacuum treatments; (vi) the chlorine atoms are coordinated to Cu ions in the nearest local shell imposed by the structure of anhydrous $CuCl_2$ with a coordination number of 4 at 2.26 Å measured by EXAFS,[37] which is consistent with the results of DFT calculation;[43−45] (vii) $CuCl_2$ is reducible by ethylene.

Cuprous Chloride (CuCl). The reduction of $CuCl_2$ by ethylene forms CuCl. The properties of CuCl are briefly summarized here: (i) it is highly volatile and causes the problems of the lifetime of the $CuCl_2$ catalysts. The vapor pressure between 230 and 350 °C is described by eq 5[46]

$$\log_{10} P(\text{mm Hg}) = -7574T^{-1} + 10.29 \quad (5)$$

(ii) when $CuCl_2$ is reduced to CuCl, the electronic structure changes from $3d^9$ to $3d^{10}$. No absorption can be observed for CuCl in the near-infrared (NIR) region,[38,47,48] and a decrease of the electron spin-flip transitions is observed in the EPR spectra;[38] (iii) the coordination number of Cl to Cu is 2;[43] (iv) it is inactive for ethylene reduction, and it cannot be reduced further at the ethylene oxychlorination reaction conditions.[47,48]

Copper Oxide Chloride (Cu_2OCl_2). Cu_2OCl_2 has been long proposed as an important intermediate in the catalytic cycle of ethylene oxychlorination.[49,50] It has been experimentally determined by EXAFS with an O coordination number of 1 and a Cl coordination number of 2, and Cu exists with an oxidation state of +2.[42] The band energy of Cu_2OCl_2 measured by UV−vis spectroscopy is similar to $CuCl_2$.

Cupric Chloride ($CuCl_2$) with Cl Vacancy. The operando X-ray absorption near-edge structure (XANES) study illustrated a mixture of $CuCl_2$ and CuCl existing in the catalysts during the reaction.[36,40,51] It was also illustrated by UV−vis-NIR that $CuCl_2$ decreases and the $CuCl_2$/CuCl ratio changes with time, as a result of the removal of Cl and forming Cl vacancies.[47] The $CuCl_2$ with a vacancy is expressed as a mixture of $CuCl_2$ and CuCl. The UV−vis-NIR spectra showed a change in the charge transfer when Cl is gradually removed. The $CuCl_2$ with a Cl vacancy has a Cl coordination number of 3 with Cu.[43] The vacancy concentration is often measured as the $CuCl_2$/CuCl ratio.

3.2. Effects of Catalyst Supports. Several supports have been applied for ethylene oxychlorination, such as alumina, silica, zeolites, activated carbon, and others.[16,22,41,52] The interaction between the $CuCl_2$ and the support surface has been recognized as an important factor to influence the catalyst activity, selectivity, and stability. The interaction between the $CuCl_2$ and support was studied by different techniques, like EPR, XRD, TPR, and solvent extraction. The main results are summarized in Table 2

EPR has been long applied as a powerful technique to study the interaction between $CuCl_2$ and various supports.[18,41,42,53,54] On $CuCl_2/Al_2O_3$ support, two different EPR signals were identified that related to different environments of the Cu(II) ion. The asymmetric or axially symmetric signal is assigned to isolated Cu(II) ions interacting with the

https://dx.doi.org/10.1021/acscatal.0c01698
ACS Catal. 2020, 10, 9299−9319

Table 2. Summary of the Different Methods Used for the Research for Supports

supports	interaction	methods	remarks	ref
γ-Al_2O_3	strong	EPR, XRD, solvent extraction	EPR identified the significant interaction between $CuCl_2$ and support. No $CuCl_2$ signals on XRD, with good dispersion of $CuCl_2$ (the most active than the others). $CuCl_2$ can be partially removed by acetone.	42, 53−55
TiO_2	relatively strong	solvent extraction	$CuCl_2$ can partly be removed by acetone; the order is γ-Al_2O_3 > TiO_2 ≥ SiO_2.	58
α-Al_2O_3	relatively weak	XRD	Cu specie is not stale. γ-Al_2O_3 > SiO_2 ≥ α-Al_2O_3. $CuCl_2$ can be easily removed by acetone.	55
SiO_2	weak	EPR, XRD, solvent extraction	Weak interaction from EPR study. $CuCl_2$ forms a particle, and it can be easily removed by acetone.	53−55

support, which is dominating on low-copper-content alumina-supported catalysts. The symmetric signal is assigned to Cu(II) ions which do not interact with the support. The symmetric one could be selectively removed by washing treatment with solvent,[41,42] demonstrating that this signal was indeed related to Cu(II) ions which did not interact with the support. The EPR study illustrated a significant interaction between the copper ions and the alumina support but not in the case of SiO_2. On Al_2O_3, Cu^{2+} ions occupied the vacancy and formed surface species stabilized by the support. The results showed that alumina is not inert, which influenced the electronic properties of Cu ions. Rouco has studied the effect of the interaction of $CuCl_2$ and the supports on three steps, namely reduction of $CuCl_2$, oxidation of CuCl, and hydrochlorination of Cu_2OCl_2 in the catalyst cycle by the TPR combined EPR.[50] The treatment of C_2H_4 results in the complete reduction of $CuCl_2$ to CuCl on SiO_2, whereas an incomplete reduction was seen on Al_2O_3. The sequential oxidation of CuCl clearly shows that oxidation to $CuCl_2$ is accomplished on Al_2O_3 but not on SiO_2.

In 1983, Zipelli et al. investigated the nature and stability of copper species on SiO_2-, γ-Al_2O_3-, and α-Al_2O_3-supported $CuCl_2$ by using XRD and reflectance spectroscopy.[55] The observed stability order of the formed complexes on these supports is the following: γ-Al_2O_3 > SiO_2 ≥ α-Al_2O_3, which indicates a strong interaction between $CuCl_2$ and γ-Al_2O_3 compared to other supports. The ethylene oxychlorination activity of Ag-promoted $CuCl_2$ decreased in an order of γ-Al_2O_3 > Kiesel gel > mordenite > α-Al_2O_3 > porous glass.[56] Rouco also illustrated a stronger salt-support interaction for $CuCl_2/\gamma$-Al_2O_3, compared to that of $CuCl_2/\alpha$-Al_2O_3 and $CuCl_2/SiO_2$ by solvent extraction, where almost 100% of $CuCl_2$ on α-Al_2O_3 and SiO_2 can be extracted, while only about 16% of $CuCl_2$ can be extracted on $CuCl_2/\gamma$-Al_2O_3.[57] $CuCl_2$ and $CuCl_2{\cdot}2H_2O$ particles were detected by XRD, and the particle size was smaller for $CuCl_2/SiO_2$ than $CuCl_2/\alpha$-Al_2O_3. Paratacamite particles were detected only on γ-Al_2O_3 but not on SiO_2 and α-Al_2O_3, due to rich OH on the γ-Al_2O_3 surface. When the catalyst was activated in HCl, paratacamite particles disappeared, and no $CuCl_2$ peaks were detected on XRD, suggesting a good dispersion of $CuCl_2$ on γ-Al_2O_3.

Similarly, Fortini et al. investigated the salt-support interactions between unprompted $CuCl_2$ and the support of γ-Al_2O_3, SiO_2, and TiO_2 by solvent extraction, where the interacted Cu with support species cannot be removed by solvents, such as acetone. The interaction is in an order of γ-Al_2O_3 > TiO_2 ≥ SiO_2, and the activity of oxychlorination of methane follows the same order.[58] They concluded that the salt-support interactions that occur on γ-Al_2O_3 and TiO_2 may give rise to stabilization of regenerable Cu(II) species and thus provide a better dispersion and resistance to deactivation.

An important consequence of the interaction between $CuCl_2$ and the support is the particle size of $CuCl_2$, which has not been well addressed so far. For the unsupported $CuCl_2$ powder, it is typically inactive for the ethylene oxychlorination. TPR in C_2H_4 indicated the reduction of $CuCl_2$ to CuCl started at higher temperatures (about 663 K), which coincides with the decomposition temperature of $CuCl_2$.[50] The larger particles increased the barrier for the reduction of $CuCl_2$. Many experimental results support the findings in which $CuCl_2$ can be stabilized on Al_2O_3[18,58] and CuCl on SiO_2.[59] The study rationalizes the importance of the effect of supports, more precisely the interaction between the Cu species and the support surface in ethylene oxychlorination. The SiO_2-supported catalysts are not active at relatively low-temperature oxychlorination reactions both in the fluidized bed and fixed-bed reactors, since the cycle between $CuCl_2$ and CuCl cannot be accomplished. Besides, the interaction between $CuCl_2$ and the support plays a virtually important role in the mobility of the Cu species. The strong adsorption on γ-Al_2O_3 reduced significantly the mobility and enhanced stability.[41,57,60]

The different supports were also used as the $CuCl_2$ catalysts and evaluated in the ethylene oxychlorination. In 1966, Todo et al. studied ethylene oxychlorination using 15 wt % of $CuCl_2$ with several different supports and reported the preferred order as alumina > silica gel > Celite.[21] The well-dispersed $CuCl_2$ shows better reducibility. Murzin and co-workers recently demonstrated an order of ethylene oxychlorination rate on $CuCl_2$ on supports of γ-Al_2O_3 > TiO_2 > H-Beta-25 > SiO_2.[61] In general, the observations are rather consistent, and the activity of $CuCl_2$ depends on its interaction with the support and follows an order of γ-Al_2O_3 > TiO_2 > H-Beta-25 > SiO_2 > α-Al_2O_3.

The superior performance of γ-Al_2O_3 might be due to its strong salt-support interaction, pore structure, high surface area, high mechanical strength, high thermal resistance, and acidity.[62] These properties ensure high catalytic activity, enhance catalyst stability, and minimize the volatility of the CuCl relative to other supports, which make γ-Al_2O_3 comparatively the best support for $CuCl_2$-based oxychlorination catalysts. Reducing the mobility of the Cu species is vitally important to avoid pellets sticking in a fluidized bed reactor. Sticking pellets can change the flow pattern of the reactor and thus disturb the stable operation. The strong adsorption of Cu species with support and adding promoters to hold a higher concentration of $CuCl_2$ can effectively minimize the pellet sticking.

Experiments found that the strong interaction between the support and the active phase plays an essential role in the ethylene oxychlorination activity.[61] Thus, it is necessary to involve the model of support in the theoretical exploitation of the active site. Louwerse et al.[39] adopted the general accepted

https://dx.doi.org/10.1021/acscatal.0c01698
ACS Catal. 2020, 10, 9299−9319

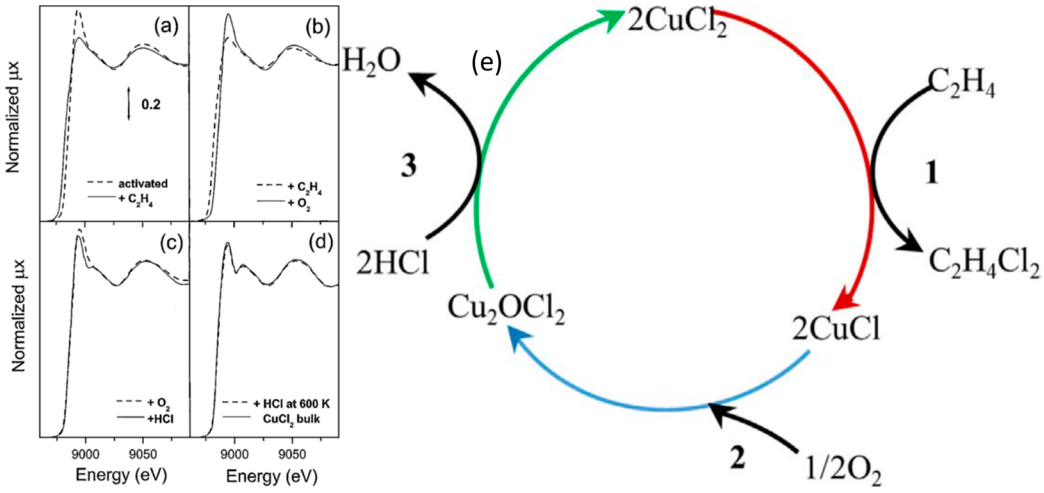

Figure 2. (a–c) Evolution of the XANES spectra of the Cu7.5 (7.5 wt % Cu, the same in the following) catalyst along the catalytic path at 500 K. (a) Effect of exposure to C_2H_4; (b) effect of exposure to O_2; (c) effect of exposure to HCl. Dashed and solid lines refer to the sample before and after the treatment, respectively. (d) The spectrum of the catalyst after successive interaction with HCl at 600 K (dashed line) compared with that of the bulk anhydrous $CuCl_2$ model compound. Reproduced with permission from ref 42. Copyright 2002 Elsevier. (e) Redox mechanism of the oxychlorination of ethylene: 1) Reduction of $CuCl_2$ by ethylene, forming EDC and CuCl. 2) Oxidation of CuCl by oxygen, forming Cu_2OCl_2. 3) Regeneration of the active $CuCl_2$ phase by hydrochlorination of the Cu_2OCl_2. Reproduced with permission from ref 68. Copyright 2018 Elsevier.

nonspinel crystal structure of γ-Al_2O_3 to investigate the structure of uncalcined copper chloride on γ-Al_2O_3. It is suggested that the adsorption Cu^{2+} and Cl^- is dependent on the surfaces of γ-Al_2O_3. They can adsorb on the (110) and (100) surfaces but not on the (111) surface for the impregnated-dried catalysts at low loadings due to its high surface energy. Moreover, the structure of fresh $CuCl_2$ catalysts at different loadings is exploited. It is found that the interaction between the support and $CuCl_2$ strongly depends on the facet of support. Compared to γ-Al_2O_3 (100), a stronger $CuCl_2$-support interaction was observed on γ-Al_2O_3 (110), owing to its stronger Lewis acidity of Al on (110). The interaction becomes weaker with the increase of the $CuCl_2$ cluster size (i.e., the loading of Cu).[44] The effect of γ-Al_2O_3 structures on ethylene oxychlorination needs to be addressed in the future. It should be noted that another important effect of the support is the acidic-base properties, which can influence the catalyst selectivity. It will be reviewed in detail in section 4.

3.3. Reaction Mechanisms. A better understanding of the reaction mechanism is of vital importance for the development of new catalysts and the improvement of current catalysts. Thus, substantial efforts have been devoted to the investigation of the reaction mechanism of ethylene oxychlorination. A Deacon mechanism was proposed at a very early stage of the process development, where HCl was oxidatively converted into Cl_2 (eq 6). Further, substitution chlorination occurs in the gas phase (eq 7), and the product may continue to undergo substitution reactions, which results in the formation of more highly chlorinated hydrocarbons. The Deacon process was developed by H. Deacon and F. Hurter[63,64] in 1868 for the recovery of chlorine and further developed by Hasenclever in 1883. Then in the 1920s, Ernst and Wahl[65] adopted the Deacon system to chlorinate hydrocarbons (methane, ethane, ethylene, and benzene) at 573–923 K. Despite the possibility of chlorinating ethylene in the Deacon reaction, a rate equation based on the Deacon-type reaction mechanism failed to fit the kinetics of ethylene oxychlorination at 180 °C.[66]

(a) Deacon reaction mechanism

$$4HCl + O_2 \rightarrow 2Cl_2 + 2H_2O \quad (6)$$

$$C_2H_4 + Cl_2 \rightarrow C_2H_4Cl_2 \quad (7)$$

(b) Three-step redox mechanism

$$C_2H_4 + 2CuCl_2 \rightarrow C_2H_4Cl_2 + 2CuCl \quad (8)$$

$$2CuCl + 1/2O_2 \rightarrow Cu_2OCl_2 \quad (9)$$

$$Cu_2OCl_2 + 2HCl \rightarrow 2CuCl_2 + H_2O \quad (10)$$

In as early as 1966, Todo et al. observed a negligible amount of Cl_2 formed on $CuCl_2$ catalysts. They proposed that the ethylene oxychlorination reaction did not go through the Deacon reaction, instead, it went through the reduction (eq 8) and oxidation as well as hydrochlorination (eqs 9 and 10) reactions.[21] Later a three-step mechanism (eqs 8–10) was proposed on $CuCl_2$ catalysts based on a Mars-van Krevelen (MvK) mechanism, where the lattice Cl participates in the reaction evidenced by the direct reduction of $CuCl_2$ by ethylene.[49,50,60] Lamberti et al. confirmed the three-step redox reaction mechanism on $CuCl_2$/γ-Al_2O_3-based catalysts by using operando X-ray absorption spectroscopy, as shown in Figure 2.[36,42,67] The XANES spectroscopy is found to be a powerful tool to measure both oxidation and coordination states of copper, which could be measured by the shift of the Cu K-edge.[42] Figure 2a indicates that interaction with ethylene leads to a redshift of the edge. Further interaction with O_2 results in an opposite shift, as shown in Figure 2b. Interaction with HCl does not significantly change the position of the edges but causes changes in the near-edge features (Figure 2c). It is generally accepted that the substitution reactions readily occur with alkane at a temperature above 400 °C, while oxychlorination of olefins prefers a three-step redox reaction (Figure 2e).[11]

Recently, the three-step MvK mechanism was further demonstrated and confirmed by a study of three individual steps using a combined UV–vis-NIR and mass spectroscopy (MS), where the evolution of the number of $CuCl_2$ with time

https://dx.doi.org/10.1021/acscatal.0c01698
ACS Catal. 2020, 10, 9299–9319

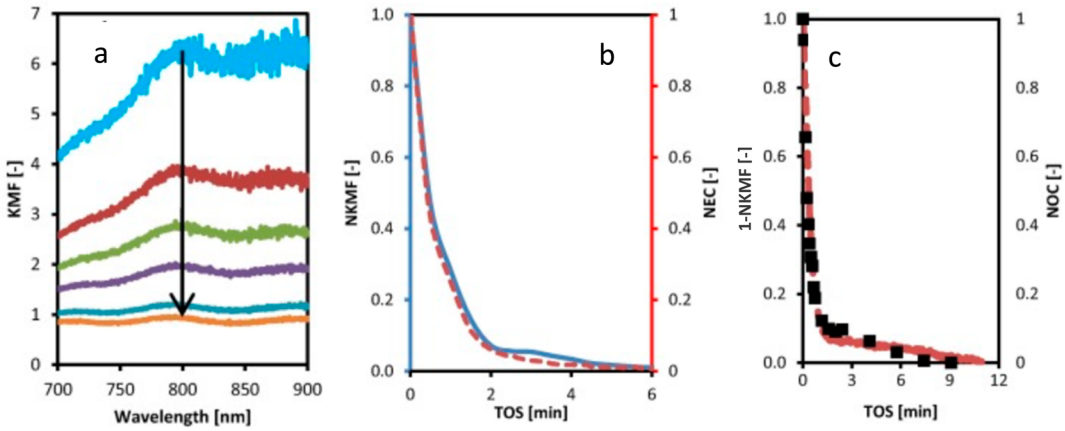

Figure 3. (a) Decrease of the Kubelka–Munk function (KMF) units in the 700–900 nm wavelength range with respect to time-on-stream (TOS) (arrow represents an increase in reaction time: 0, 30, 60, 90, 210, 450 s) in the reduction step. (b) Normalized ethylene conversion (NEC) and the normalized Kubelka–Munk function (NKMF) vs TOS. Catalyst: Cu5.0; reduction step reaction conditions: $P_{C_2H_4}$ = 0.1 atm, T = 230 °C, (c) Normalized oxygen conversion (NOC) and (1-NKMF) vs TOS. Catalyst: Cu5.0; oxidation step reaction condition: P_{O_2} = 0.1 atm; T = 230 °C; P_{Total} = 1 atm. Reproduced with permission from ref 47. Copyright 2017 Elsevier.

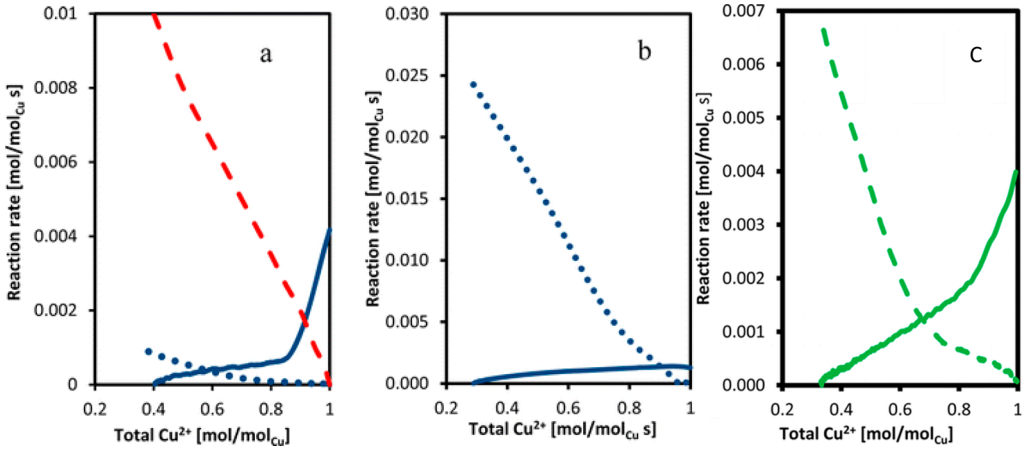

Figure 4. (a) Reaction rate of the reduction (blue —) and oxidation (blue ●●●) steps of the Cu5.0 catalyst and the proposed oxidation reaction rate (red — —) in an ideal catalyst. (b) The reaction rate of the reduction (blue —) and oxidation (blue ●●●) steps of K1.54Cu5.0. (c) The reaction rate of reduction (green —) and oxidation (green — —) steps on the Ce1.0Cu5.0 catalyst. Reduction step reaction conditions: $P_{C_2H_4}$ = 0.1 atm, T = 230 °C, P_{Total} = 1 atm, and oxidation step reaction conditions: P_{O_2} = 0.1 atm, T = 230 °C, P_{Total} = 1 atm. Copyright 2016 American Chemical Society.

was investigated.[47,48,68] The Kubelka–Munk function (KMF) at 793 nm is sensitive to the d–d transition band of $CuCl_2$. CuCl with the electronic configuration of $3d^{10}$ does not exhibit a d–d band transition. Therefore, a decrease of $CuCl_2$ on the catalyst, accompanied by an increase of CuCl, results in a decreasing KMF as the reduction proceeds. As shown in Figure 3, the KMF decreased with the reduction of $CuCl_2$ to CuCl by ethylene. The KMF increased reversibly with the oxidation of CuCl to Cu_2OCl_2 by oxygen. The relative change in the Normalized Kubelka–Munk function (NKMF) with time followed the changes in the relative Normalized ethylene conversion (NEC) in the reduction step and also followed the relative changes in the reducible $CuCl_2$ (Figure 3) suggesting lattice Cl in $CuCl_2$ is responsible for ethylene oxychlorination. The change in KMF units with time during the transient oxidation is opposite to the transient reduction. The changes in $CuCl_2$ are reversible in the reduction and oxidation steps. Combining the fast hydrochlorination step, the three steps form a cycle of the ethylene oxychlorination (Figure 2e).

It should be noted that the oxychlorination mechanism depends on the catalyst. For the alumina-supported $CuCl_2$ catalyst, a three-step mechanism is dominating and has relatively low adsorption strength of EDC, which lead to the highest EDC selectivity among all the oxychlorination catalysts reported so far. For other catalysts like rare-earth metal oxides or chlorides, they served as the bifunctional catalysts in the direct VCM production from ethylene oxychlorination, and the oxychlorination follows a Langmuir–Hinshelwood surface reaction mechanism. For example, with the Ce-based catalyst, the catalyst surface is found to contain CeOCl, while the bulk phase is CeO_2, regardless of the starting material $CeCl_3$, CeOCl, or CeO_2. Pérez-Ramírez and co-workers have performed the kinetic study and proposed a reaction mechanism on the CeO_2 surface by combining DFT with steady-state experiments and temporal analysis of products (TAP).[34] The two steps of ethylene oxychlorination and EDC dehydrochlorination can be integrated into a one-pot process on a bifunctional catalyst, which catalyzes the surface ethylene

https://dx.doi.org/10.1021/acscatal.0c01698
ACS Catal. 2020, 10, 9299–9319

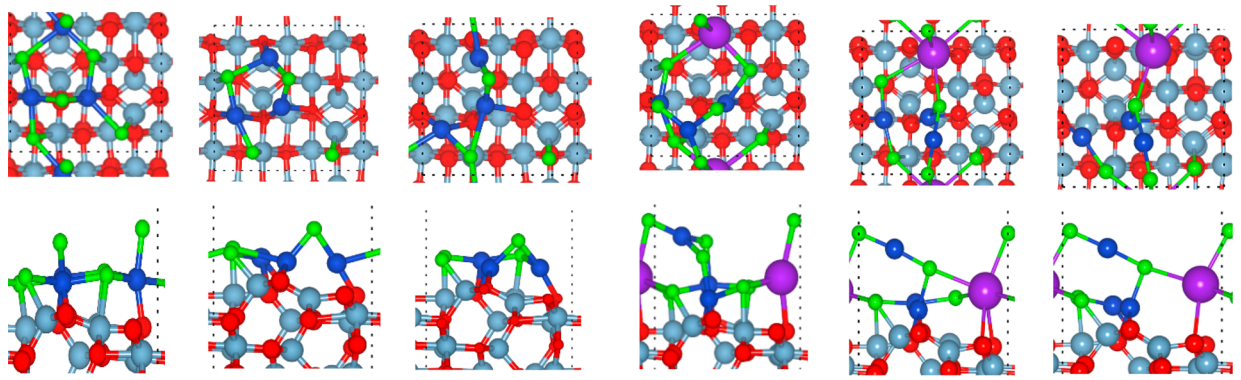

Figure 5. Top views and side views of the structure of neat catalysts and potassium-promoted catalysts with different Cl/Cu ratios. Atom colors: O = red, Al = livid, Cu = blue, K = purple, Cl = green. Reproduced with permission from ref 44. Copyright 2020 Elsevier.

oxychlorination to EDC and dehydrochlorination of EDC to VCM.[30] It opens a new door for the optimization and the intensification of the current two-step VCM process into one single step. All the rare-earth metal oxides or chlorides catalyze both EDC and VCM production, instead of selective EDC production.

For the three-step mechanism, the reduction, oxidation, and hydrochlorination are sequential reaction steps. Lamberti and co-workers suggested the CuCl oxidation was the rate-determining step (RDS) on neat Cu, and K-promoter changes the RDS to ethylene reduction steps based on the results of operando X-ray absorption spectroscopy.[35,36,40]

We have recently developed a virtual approach using a rate-diagram to elucidate the active sites, illustrate the rate-determining step, and predict the reaction rate and Cu oxidation state at the steady state.[48] The rate of the transient reduction and oxidation steps, as well as the steady-state kinetics of the ethylene oxychlorination reaction including the precise evolution of the catalytically active component, was measured by combined operando UV−vis-NIR and mass spectroscopy. In the rate-diagram, the reaction rates of the reduction and oxidation steps on the catalysts are plotted as a function of the concentration of $CuCl_2$ in Figure 4. At the steady state, the reduction and oxidation reaction rates are identical, represented as the cross point of the two curves. In this respect, the rate and the Cu oxidation state corresponding to the interaction point represent the steady-state rate and Cu oxidation state at the given reaction conditions. For example, the rate-diagram of the $CuCl_2/Al_2O_3$ catalyst without promoters as shown in Figure 4a illustrated that the oxidation rate is relatively low, and the reduction rate is relatively high. As a result, the steady-state $CuCl_2$ concentration and the reaction rate are relatively low, which is consistent with the experimental measured $CuCl_2$ values.[48] The low $CuCl_2$ and high CuCl cause Cu loss and deactivation due to the high volatility of CuCl. The reoxidation of reduced catalysts is the RDS, which is in good agreement with other observations.[49,51] The industrial catalysts are always promoted by alkaline metals, alkaline-earth metals, or rare-earth metals for practical use. As shown in Figure 4b,c, the promoters such as K and Ce improved the oxidation of the reduced Cu catalysts and thus reduced the concentration of CuCl.

The rate-diagram is a powerful tool to predict the dynamic active sites by taking into account the kinetic balance of the three steps in the catalytic cycle to predict the steady-state $CuCl_2$ concentration and the reaction rate. It leads to an important conclusion that the steady-state rate depends on not only the redox reaction rate but also the number of active sites, namely the concentration of $CuCl_2$ and CuCl under working conditions, instead of the initial oxidation state. Moreover, the rate-diagram can guide the catalyst design to tune the reduction and oxidation rates to remarkably improve the activity and stability. The rate-diagram suggests that the desired $CuCl_2$-based catalysts should have a much higher oxidation rate than the neat Cu catalysts but without lowering too much the reduction rate, in order to achieve a higher rate and $CuCl_2$ concentration, thus active and stable catalysts, as illustrated by the red dashed line in Figure 4a. The promoter is a good choice to achieve the goal such as K- and Ce-promoted catalysts shown in parts b and c, respectively, of Figure 4. The approach of the rate-diagram will be applied to analyze the detailed effect of promoters on the catalyst performance in the role of promoters in section 3.4. Therefore, it is concluded that the RDS varies at different reaction conditions, supports, and additives, although it generally follows the three-step redox mechanism.

3.4. Active Sites in $CuCl_2/\gamma$-Al_2O_3-Based Catalysts.

Large efforts have been devoted to understanding the Cu species on alumina by various techniques such as EPR,[50] EXAFS, and UV−vis-NIR.[37,38,42,67] Active sites are entities on a catalyst surface to which molecules bind, for a reaction to occur. They directly participate in a catalytic reaction cycle[69] and are energetically favored to support the reaction. The nature and reactivity of active sites of the oxychlorination catalysts have been intensively investigated.[16,36−38,55,70−73] However, the identified active sites in the literature are rather controversial. Here, we review all the proposed active sites and the experimental evidence, try to make a critical analysis, and unify the active site at the end.

TPD results found the ethylene can be chemisorbed on $CuCl_2$ at low temperatures.[49,50,57] Pulse[40] and direct reduction of $CuCl_2$ by ethylene revealed the highly dispersed $CuCl_2$ is active for the reaction. It was also revealed that a high $CuCl_2$ concentration in the working catalyst could improve the

https://dx.doi.org/10.1021/acscatal.0c01698
ACS Catal. 2020, 10, 9299−9319

activity, selectivity, and stability by the transient and steady-state operando kinetic studies.[48] Therefore, it was generally accepted that the active phase is a highly dispersed $CuCl_2$.[37,38,50,57,58] Besides, it has been reported that the $CuCl_2$ can disperse spontaneously onto the surface of the support and form a monolayer type structure because the monolayer is a thermodynamically stable form by Xie et al.[74] With the help of DFT, a molecular view of the active site structures without a promoter and with the K-promoter is illustrated in Figure 5.[44] The monolayer of $CuCl_2$ is epitaxially bonded with the alumina surface, where Cu is bonded with O, and Cl is bonded with Al in the alumina. This also pointed out the importance of the support surface on the properties of the epitaxially bonded $CuCl_2$ layer. Moreover, Figure 5 illustrated the evolution of the active sites from the $CuCl_2$ to $CuCl_2$-vacancy and the end of CuCl. The K promoter forms a complex layer with $CuCl_2$. Due to a larger size of K, it results in a distortion of the $CuCl_2$ layer, which influences its activity.

On the contrary, Xie et al.[75] observed that two active sites with different reactivities existed on the support. The first was described as $CuCl_2$ with four coordination in a square planar configuration, whereas the second is a five- or six-coordinated Cu species formed from the adsorption of HCl. They further explained that the first site is more active than the second site due to stereo- and electronic effects that inhibit the adsorption of ethylene.

Although the $CuCl_2$ has been generally identified as the main active site, the three reaction steps might require different sites. Arcoya et al. studied for the first time the reactions for three individual steps in 1982 and reported that the reoxidation of reduced Cu catalysts is a slow process and the K promoter could enhance the oxidation. They found that the ethylene oxychlorination reaction rate was proportional to the amount of $CuCl_2$ in the $KCuCl_2/\alpha$-Al_2O_3, and $CuCl_2$ was the main active site. We also observed that the $CuCl_2$ reduction and CuCl oxidation are proportional to the amount of $CuCl_2$ and CuCl as shown in Figure 4.[47,48] Lamberti and co-workers investigated the evolution of catalyst activity and of the average oxidation state of copper in the catalyst followed under real-time working conditions by using operando XANES spectroscopy.[36,51,72] The technique allows a measurement of the $CuCl_2$ and CuCl in real-time. Both $CuCl_2$ and CuCl existed under the working reaction conditions. Moreover, the concentration of $CuCl_2$ and CuCl was highly dynamic in the temperature-programmed reactions. We recently also demonstrated the $CuCl_2$ concentration changes with time by the combined UV–vis-NIR and MS. The technique allows us to measure the timely and spatial distribution of $CuCl_2$ in the reaction.[47] The changes in ethylene conversion are closely related to the $CuCl_2$ concentration change (Figure 6). For the neat $CuCl_2/\gamma$-Al_2O_3 catalyst, the $CuCl_2$ was mostly reduced, and the remaining 40% $CuCl_2$ was the copper-aluminate species and a small amount of CuCl. It caused catalyst deactivation due to Cu loss.

The Cu oxidation state increased with increasing the oxygen pressure (Figure 6). Both $CuCl_2$ and CuCl or more precisely the Cl vacancy always coexists but varies on the reaction conditions and catalysts.[47,48] Therefore, the active site is the $CuCl_2$ with the Cl vacancy. Importantly, the active site is highly dynamic under working conditions. It points out the importance of controlling the $CuCl_2$/CuCl concentration under working conditions to achieve a stable catalyst, through tuning the reaction conditions and catalyst composition.

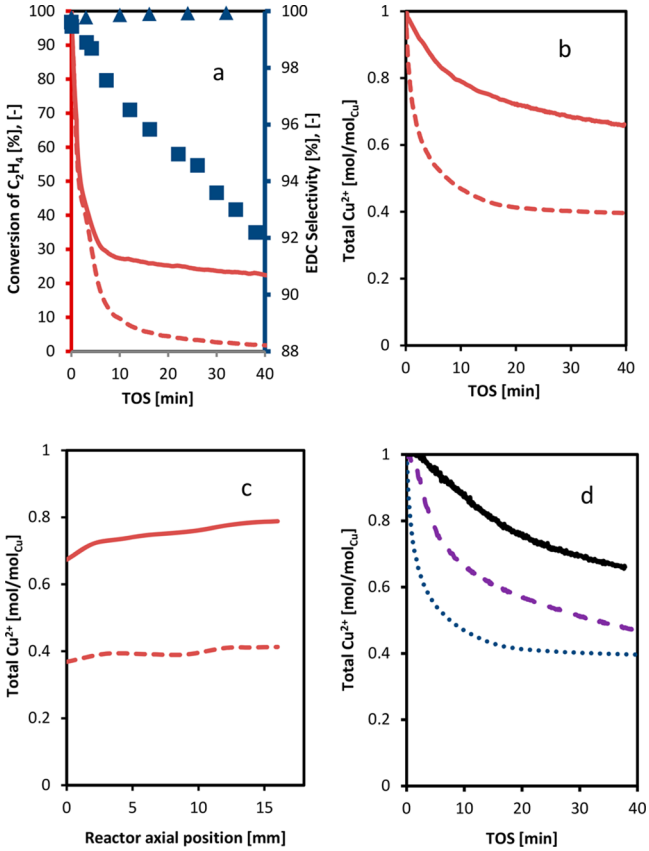

Figure 6. a) C_2H_4 conversion and EDC selectivity vs TOS (reaction conditions I (▲) and II (■)), b) total Cu^{2+} during TOS by keeping the UV–vis-NIR probe at the top of the catalyst bed, c) total Cu^{2+} vs reactor axis at 60 min of the total catalytic reaction [steady-state reaction condition I (—): $P_{C_2H_4}$ = 0.009 atm, P_{O_2} = 0.0189 atm, P_{HCl} = 0.0189 atm, T = 230 °C, P_{Total} = 1 atm, and steady-state reaction condition II (---): $P_{C_2H_4}$ = 0.009 atm, P_{O_2} = 0.0045 atm, P_{HCl} = 0.0189 atm, T = 230 °C, P_{Total} = 1 atm], d) total Cu^{2+} during TOS by keeping the UV–vis-NIR probe at the top (●●●), middle (---), and bottom (—) of the catalyst bed at reaction condition II; catalyst: Cu5.0. Reproduced with permission from ref 47. Copyright 2017 Elsevier.

Based on the critical analysis of the experimental and theoretical observation in the literature, we can conclude the active sites under working conditions, where there is no single active site, and the $CuCl_2$ with vacancies, CuCl, and Cu_2OCl_2 are the active sites since three reaction steps require different active sites. The dominating active sites depend on the RDS. The CuCl is dominating when the oxidation step is the RDS, while $CuCl_2$ with vacancies is the dominating active site when the reduction is the RDS.

3.5. Promoters and the Nature of the Promotion.

Although $CuCl_2/\gamma$-Al_2O_3 exhibits good activity for ethylene oxychlorination compared to other catalysts, it suffers a fast deactivation due to agglomeration and vaporization of CuCl. As evidenced by the previous research, there are two types of Cu-species on the catalyst: the inactive Cu-aluminate and the active-supported $CuCl_2$. The dopants can increase the fraction of the active phase by first filling in the vacancies of alumina. Quantitative analysis of EXAFS and XANES shows that all dopants can contribute more or less efficiently in increasing the fraction of the active copper species, and the efficiency is proportional to the ability of the corresponding cations to

https://dx.doi.org/10.1021/acscatal.0c01698
ACS Catal. 2020, 10, 9299–9319

compete with $CuCl_2$ occupying the vacancies.[35] Therefore, the industrial catalysts are typically promoted to maintain and enhance the activity and stability of $CuCl_2/\gamma$-Al_2O_3. Based on the promoter chemical identity, the promoters can be classified into alkali metals (K, Na, Li, and Cs),[40,47,49,57,60,68] alkali-earth metals (Mg, Ca, Sr, etc.),[40,60,76,77] and rare-earth metals such as La, Ce, Pr, etc.[17,35,40,48,57,60,77−81] Based on the number of promoters employed in one catalyst, the promoters can be classified as mono-, bi-, and multipromoters.

3.5.1. Monopromoters. Alkali Metal Chlorides. The K promoter presents commercial oxychlorination catalysts[82−91] and has been studied extensively.[35,36,40,52,57,72,92−95] The first reported K promoter for the $CuCl_2$ catalyst for ethylene oxychlorination was back in 1966.[96]

Arcoya et al. for the first time in 1982 demonstrated that the oxidation reaction rate doubled upon the addition of K to the catalyst using the α-Al_2O_3 support.[49] It was identified that the oxidation is the RDS on $CuCl_2/\gamma$-Al_2O_3, while K shifts the RDS to the reduction step since K significantly enhances the oxidation of the catalyst and renders the reduction reaction.[36] It should be noted that the conclusion was drawn solely based on the individual steps, ignoring the competitive reactions of the three steps under working conditions. The operando study is necessary to elucidate the nature of the promoter under working conditions. Muddada et al.[40] performed an *in situ* XANES study of the temperature-programmed ethylene oxychlorination. Both the O_2 conversion represented as activity and the Cu^{II} fraction of the K3.6Cu5.0 catalysts, where the number in the catalyst code represents the weight fraction of components, were measured and compared to the Cu5.0 catalysts, as shown in Figure 7. The starting temperature of the

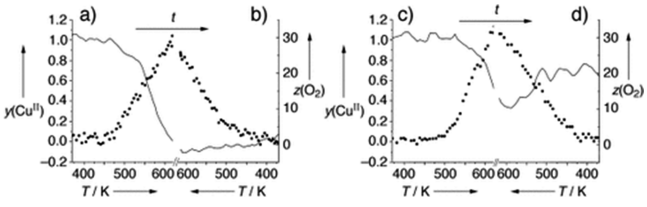

Figure 7. a) O_2 conversion (representative for the catalyst's activity; z, full dots, right axis) and Cu^{II} fraction (y, full line, left axis) for Cu5.0 during temperature ramp-up. b) As diagram (a) but for the temperature ramp-down. c) and d) Equivalent presentations to (a) and (b) for K3.6Cu5.0. The time axis runs in all diagram parts from left to right. $y(Cu^{II}) = 1-y(Cu^{I})$, where $y(Cu^{I})$ has been determined by the relative intensity of the first derivative maximum at 8982 eV compared to the value obtained on a totally reduced sample. Reproduced with permission from ref 36. Copyright 2002 Wiley-VCH Verlag GmbH.

reaction is higher on Cu5.0 (480 K) than K3.6Cu5.0 (520 K), suggesting a lower activity on the K-promoted catalyst. The pulse experiments indicated also the rate of $CuCl_2$ reduction by ethylene is lower on K3.6Cu5.0 than Cu5.0. Contrary, the activity of CuCl oxidation is higher on the K-promoted catalyst than the neat Cu. The XANES results revealed that CuCl is dominating on Cu5.0 owing to the oxidation of CuCl is the RDS, while $CuCl_2$ is dominating on K3.6Cu5.0 due to the reduction of $CuCl_2$ being the RDS. The results illustrate that the addition of K favors the Cu^{II} state, leading to an increase in the oxidation rate or a decrease in the reduction rate.

Applying the rate-diagram analysis to the typical K-promoted $CuCl_2/Al_2O_3$ catalyst (K1.54Cu5) shown in Figure 4, the CuCl oxidation rate is significantly higher, while the $CuCl_2$ reduction is lower than the neat Cu catalyst.[47] As a result, at the steady state, the $CuCl_2$ concentration was much higher than the neat Cu catalyst, while the reaction rate was not significantly affected. It rationalized why K is the most applied promoter in the industry.

In general, the presence of K in the catalysts increased the apparent activation energy of the oxychlorination reactions.[49,97] DFT calculations confirmed the formation of a mixed K_xCuCl_{2+x} salt (Figure 5) on the alumina surface and demonstrated that KCl reduced the interaction between the support and the active phase. It supports the experimental observation that the K promoter increased the $CuCl_2$ concentration to 0.81 mol/mol_{Cu}, from 0.56 mol/mol_{Cu} of the neat copper chloride catalysts.[48] The DFT study suggested a complex structure of Cu_3KCl_7 on γ-Al_2O_3, similar to the reported salt. Charge density difference analysis elucidates that the electron transfer between K and neighboring Cu and Cl atoms results in substantial electron accumulation around the Cu and chlorine atoms and the decline of the Bader charge of Cl and Cu. Thus, it raised the formation energy of Cl vacancy and facilitated the oxygen adsorption, dissociation, and CuCl oxidation upon the addition of KCl. The formation energy of Cl vacancy increases with the decreasing of Cl/Cu ratios on both unprompted and K-promoted catalyst surfaces, which attributes to the decline in the Cl charge at lower Cl/Cu ratios. The effects of K on the oxychlorination catalysts from observations of different researchers could be concluded as the following:

1) K forms mixed salts (CuK_xCl_{2+x}) with the base catalyst, which modifies the redox properties of the catalyst and the reducibility of the active $CuCl_2$ and facilitates the regeneration of Cu(II) from Cu(I). The RDS is changed from CuCl oxidation to $CuCl_2$ reduction due to the addition of K.[35,36,40,72]
2) K causes an increase in the apparent activation energy. The effect of K on activity depends on the temperature, that is, a negative effect when the temperature is lower than 525 K and a positive effect at a temperature higher than 525 K.[57]
3) K is selectively adsorbed on tetrahedral Lewis Al^{3+} sites of the γ-Al_2O_3 surface, which modifies the physical and electronic properties of γ-Al_2O_3. This effect is pronounced with an increasing molar concentration of K.[93]
4) The addition of K reduces the surface area of the active phase.[72]
5) K reduces the volatility of CuCl and therefore makes the catalyst more stable.

In addition to K, research on other promoters has also attracted great interest. It has been found that Cs affects the catalyst and support similarly to K, albeit to varying degrees.[40,72,76] In contrast to K and Ce, Li increases the dispersion of the active phase and does not form a mixed salt with $CuCl_2$.[40,72,93]

Muddada et al.[40] performed *in situ* XANES coupled with temperature-programmed reactions on the $CuCl_2$-based catalyst doped with K, Cs, and Li promoters. At the steady state, all dopants had a positive effect on the available fraction of the active $CuCl_2$ phase. However, the activity test revealed that not all dopants positively influence the ethylene chlorination reaction. The detailed activity was not measured

https://dx.doi.org/10.1021/acscatal.0c01698
ACS Catal. 2020, 10, 9299−9319

but was approximately estimated as the activity tendency based on the $CuCl_2$ reduction temperature, and a lower starting temperature accounts for higher activity.

There are two other factors added to the complexity of the promoter effects, namely dependence of the promoter loading and the support. The effect of the K promoter on the activity of the oxychlorination reaction depends on the loading of the relative loading of K. A "volcano curve" between the K loading and the activity was observed where small amounts of K increased the activity, whereas excess K diminished it.[49,98−100] The effect of the promoter on the activity of oxychlorination depends also on the support. For $CuCl_2/Al_2O_3$, NaCl and KCl have a significant positive effect on ethylene conversion on α-Al_2O_3, that is there is a substantial increase in conversion for the α-Al_2O_3 and SiO_2, while the promoting effect for γ-Al_2O_3 is less pronounced.[49]

Therefore, the classification of the promoters into two types in terms of the RDS might be not universal but depends on the promoter loading as well as the supports. It needs a more systematic study to gain a better understanding of the promoter effect.

Rare-Earth Metal Chlorides. La is one of the most used promoters in industrial catalysts. La is traditionally considered as a structural additive in many patents where La makes $CuCl_2$ highly dispersed and prevents catalyst particles from sintering and agglomerating or sticking, especially in fluidized-bed operations.[41,101−103] Ce has been found to have a similar effect on the $CuCl_2$-based catalysts.[104] La is often added to K-promoted industrial oxychlorination catalysts though in a small amount.[35,40,41,103] It has also been found that La preferably occupies the octahedral vacancies of γ-Al_2O_3; as a result, the amount of the dispersed active phase of the catalyst is increased significantly, and even 100% active phase can be available. It significantly increases the dispersion of $CuCl_2$ and enhances the Brønsted acidity of the support.[35,40,76,103] Rouco[57] found that the La promoter accelerated the reaction rate without changing the apparent activation energy with a feed molar ratio (C_2H_4:HCl:O_2) of 1:1.8:1.1 at temperatures ranging from 185 to 240 °C, which is different from K, suggesting a purely structural promotion.

However, a large body of experimental results pointed out that La does not serve only as the structure additive but also significantly alters the surface reactions through the chemical promotion. We recently found that La[68] and Ce[48] promoters significantly enhanced both the reduction of $CuCl_2$ and oxidation of CuCl. In the rate-diagram, as shown in Figure 4, the Ce promoter increased the steady-state reaction rate, but there was not a significant increase in the concentration of $CuCl_2$.[48] It is consistent with the observation from operando experiments that La and Ce increased the $CuCl_2$ reduction rate, and the reduction was the RDS of the oxychlorination reaction where the CuCl was dominating.[40] La showed a similar promotion effect as Ce but with a less degree since La-promoted catalysts enhanced HCl adsorption and then suppressed the reaction to a certain degree. A negative reaction order with respect to HCl was found on La-promoted Cu catalysts.[68] This could explain the observed strong temperature dependence of La promotion effects on the activity. The rate of ethylene oxychlorination of La-promoted catalysts is similar to neat Cu at 503 K and much higher than neat Cu catalysts at 573 K. The adsorption became weaker at a higher temperature.[77] This can also explain the observation of Villadsen and Livbjerg that La increased the rate of sublimation of CuCl, possibly increasing the CuCl concentration, which is an undesirable effect in terms of catalyst stability.[105] Dotson suggested that this undesirable effect occurs because La forms strong chloride complexes with Cl and, thus, competes with CuCl for Cl to form neutral Cu species, which sublimes faster than CuCl.[60] From the rate-diagram analysis, La and Ce enhanced both the reduction and oxidation rate thus leading to a relatively high concentration of CuCl at the steady state, and it can enhance the sublimation of CuCl.

Zhitao et al.[80] attributed the positive impact of Ce on the existence of surface cerium oxide, which supplied oxygen for the oxidation step. XRD results show that cerium chloride was transformed into cerium oxide at the beginning of the reaction. Li et al.[106] detected that three different species of CeO_2 existed (i.e., dispersed CeO_2, small aggregated crystalline CeO_2, and large CeO_2 particles) with the increase of Ce loading, where the small aggregated crystalline ceria species was highly active. The promotion effect of Ce was attributed to the formation of O_2^- or O^-, which enhanced the oxidation of CuCl and provided extra weak acidic sites for the rupture of the C−H bond in ethane. CeOCl and $CeAlO_3$ species may cause the deactivation. A highly active and stable Ce-promoted $CuCl_2$ catalyst was developed, which achieved about 87% and 66% higher activity than unpromoted catalysts and K-promoted catalysts.[48] It is found that the various promoters play distinct roles in the reaction. The effects of rare-earth metal oxides or chlorides on the oxychlorination catalysts from observations of different researchers could be concluded as the following:

1) La and Ce increased the dispersion of $CuCl_2$ on the surface[72] and increased the reducibility of the active $CuCl_2$.
2) La[68] and Ce[48] modified the redox properties of the catalyst, increased both the reducibility of the active $CuCl_2$, and facilitated the reduction of Cu(II) to Cu(I). The oxidation step is the RDS.[40]
3) This type of promoter is immobile and often used to stabilize the Cu catalyst and prevent aggregation.

Alkaline-Earth Metal Chlorides. Mg is the most reported promoter in alkaline-earth chlorides, but it has been more often applied in catalysts for ethane oxychlorination. In ethylene oxychlorination, Mg behaves similarly to La and Ce promoters, which increases the reaction rate,[77] by enhancing both reduction and oxidation rates. The oxidation step is also the RDS, and CuCl is dominating in the steady-state operation. The addition of Mg and Ca promoters gave a good rate with high selectivity larger than 99%.[56]

In summary, the neat Cu has a high rate of $CuCl_2$ reduction and a lower rate of CuCl oxidation leading to CuCl dominating at the steady-state operation. The promoter greatly alerted Cu properties and activities. Based on the measured $CuCl_2$ concentration at the temperature region of the typical ethylene oxychlorination reaction condition, the dopants can be classified into two types, where type I consisted of La, Mg, and Li, while type II consisted of K and Cs. For the type I catalysts, the RDS is the oxidation step, where the CuCl is dominating on the catalyst, while type II catalysts change the RDS to the reduction step, where $CuCl_2$ is dominating.[40] The reducibility of these catalysts is measured by pulse reaction of ethylene followed by La10.9Cu5.0 > Mg1.9Cu5.0 > Li0.5Cu5.0 > Cu5.0 > K3.1Cu5.0 > Cs10.4Cu5.0. However, the steady-state activity did not follow the same order of the reduction; it followed an order of Ce11.0Cu5.0 > Cu5.0 >

https://dx.doi.org/10.1021/acscatal.0c01698
ACS Catal. 2020, 10, 9299−9319

Mg1.9Cu5.0 > La10.9> K3.1Cu5.0 > Li0.5Cu5.0 > Cs10.4Cu5.0. The results pointed to that the effects of promoters on the oxychlorination reaction are highly dynamic and complicated based on the kinetic balance of three steps in the catalytic cycle. Here we redefine the categories, and the promoter can be divided into two types. The alkaline metal promoters increased the CuCl oxidation rate and reduced the $CuCl_2$ reduction rate leading to $CuCl_2$ dominating and slightly increased the reaction rate at steady-state operation, typically as one shown in Figure 4b. Class II is the rare-earth and alkaline-earth metal promoters that enhanced both the reduction and oxidation rate leading to CuCl dominating but a significantly increased reaction rate at the steady-state operation, typically shown in Figure 4c. Therefore, the monopromoter could not meet the requirement of more active and stable catalysts simultaneously. The copromoter is a good solution to achieve the goal.

3.5.2. Bi- and Multipromoters. Commercially available catalysts usually contain more than one promoter,[82−84,107−110] and several studies have explored copromoting oxychlorination catalysts.[41,54,57,77,106,111] The most often reported copromoter is the K−La system.[35,41,101−103] It is reported that the $CuCl_2$ catalyst copromoted by La and K improved the activity and stability at 397 °C.[41] It has been demonstrated that the adding of La to K-promoted catalysts enhanced the stability by inhibiting the segregation of K.[57] However, it was found that the catalyst deactivated due to carbon formation and loss of Cu active species at 500 °C over γ-Al_2O_3-supported K/La/$CuCl_2$ after 40 h on stream.[103] We found a synergy effect of K and La on both $CuCl_2$ reduction and CuCl oxidation. However, the synergy effect did not lead to a significant increase in the overall reaction rate, due to the strong adsorption of HCl.[68] Arcoya et al.[49] revealed that the presence of rare-earth metal chlorides such as Ce, Nd, and Pr in K-$CuCl_2$ catalysts increased the conversion.

Multiple promoters are only reported in the patents. A small number of noble metals or noble metal chloride (Eu, Pd, Au)-promoted $Cu_{4.5}Mg_{1.5}K_{0.4}$ catalysts can increase the activity and selectivity of ethylene oxychlorination and reduce the oxidation of the products to CO_x.[112] The activity follows an order of $Cu_{4.5}Mg_{1.5}K_{0.4}Au_{0.005}$ > $Cu_{4.5}Mg_{1.5}K_{0.4}Ru_{0.01}$ ≈ $Cu_{4.5}Mg_{1.5}K_{0.4}Pd_{0.01}$ > $Cu_{4.5}Mg_{1.5}K_{0.4}$ (B). Ag was also found to be a good promoter.[56]

4. REACTION PATHWAYS AND ACTIVE SITES FOR BYPRODUCT FORMATION

The $CuCl_2$ catalysts are very selective to EDC, and typical selectivity is higher than 98%. The selectivity depends on the catalysts, reaction conditions (like temperature and feed composition), and reactor type.[113] The exposing acid sites (Brønsted and Lewis type) on the γ-Al_2O_3 support are one main reason for the side reactions. While the exposing acid sites can be modified by adding proper promoters, the side reaction can be prohibited further. The typical yields of the byproducts in both industrial fixed and fluidized bed processes of ethylene oxychlorination are presented in Table 3:[114]

Although the selectivity of 1,2-EDC is high, it still has environmental and economic benefits to further improve the selectivity. A number of undesirable byproducts are produced in the industrial plants,[16] for example, vinyl chloride (VCM, C_2H_3Cl), 1,1,2-trichloroethane (TEC, $C_2H_3Cl_3$), ethyl chloride (EC, C_2H_5Cl), trichloroethylene (TCE, C_2HCl_3), 1,1-dichloroethane (1,1-EDC, $C_2H_4Cl_2$), chloroacetaldehyde (ACC, C_2H_3OCl), carbon tetrachloride (CCl_4), 1,2-dichloroethylene (DCE, $C_2H_2Cl_2$), methyl chloride (CH_3Cl), 1,1,2,2-tetrachloroethane ($C_2H_2Cl_4$), CO/CO_2, etc. The byproducts can be classified into two main groups, namely organochlorine compounds and deep oxidation products CO and CO_2. The process can be characterized by "chlorine selectivity" and "ethylene selectivity" considering Cl conversion in HCl to EDC and other organic compounds involved chloride and carbon conversion in ethylene to organochlorine compounds and CO_x. In the best-operating regimes, chlorine selectivity to EDC exceeds 99%; ethylene selectivity to organochlorine compounds is 96−98%, depending on the oxidizer that is used (concentrated or atmospheric oxygen).[115]

Table 3. Yield of Byproducts, mol %, in Industrial Ethylene Oxychlorination Processes[114]

byproducts	fixed-bed technology	fluidized-bed technology
CO_2 + CO	0.5−0.7	1−2
1,1,2-trichloroethane	0.1−0.3	0.3−0.8
trichloroacetadehyde (chloral)	0.3−0.5	0.1−0.3
trichloromethane (chloroform)	0.1−0.2	0.1−0.2
tetrachloromethane	0.1−0.2	0.1−0.2
dichloroethylens	≤0.1	≤0.1

The oxychlorination reaction network is rather complex as numerous routes, such as substitution, addition, elimination, and oxidation, leading to a series of chlorinated and oxidized products, can take place.[22,73,116−120] Based on the critical analysis of the literature, the reaction pathways of different organochlorine products are proposed in Figure 8.

The byproducts except for ethyl chloride (EC) are formed from the second reaction of EDC, as shown in Figure 8. The Cu active sites, as well as the active sites on alumina, catalyze the secondary reactions. Catalysis for byproduct formation in ethylene oxychlorination was investigated mostly in laboratories in Russia, which has been well summarized by Flid including many Russian references.[114,115] Here we critically review the progress in the study of byproduction formation in the ethylene chlorination on Cu catalysts in terms of the reaction mechanism and site requirement, by combining Flid's work and other literature.

EC and VCM by Hydrochlorination and Dehydrochlorination. EC is formed by the ethylene hydrochlorination reaction, following a first-order with respect to ethylene and hydrogen chloride, and is inhibited by water vapor. Higher water pressure can suppress the formation of EC.[114] The reaction occurs at the same site of the oxychlorination. The EC can undergo dehydrochlorination to ethylene catalyzed by acidic sites.[121]

The formation of chlorogenic byproducts in the ethylene oxychlorination process has been summarized by Flid.[114] The dehydrochlorination reaction is a crucial reaction step for the byproduct formation, which is typically catalyzed by acidic sites.[49,73,118,119,122] Muddada et al.[76,77] have performed a systematic study of the conversion of EDC on various supports and catalysts and correlated to the different active components, such as alumina, chlorinated alumina, $CuCl_2$, CuCl, Cu_2OCl_2, and promoted $CuCl_2$. The authors studied Brønsted and Lewis sites of catalysts using the IR spectra of CO dosed on the catalyst. The Al^{3+}···CO and Al−OH···CO adducts caused blue shifts of ν(CO), which usually is in the 2230−2180 cm^{-1} and in 2155−2175 cm^{-1} ranges, respectively. In this way, the role

https://dx.doi.org/10.1021/acscatal.0c01698
ACS Catal. 2020, 10, 9299−9319

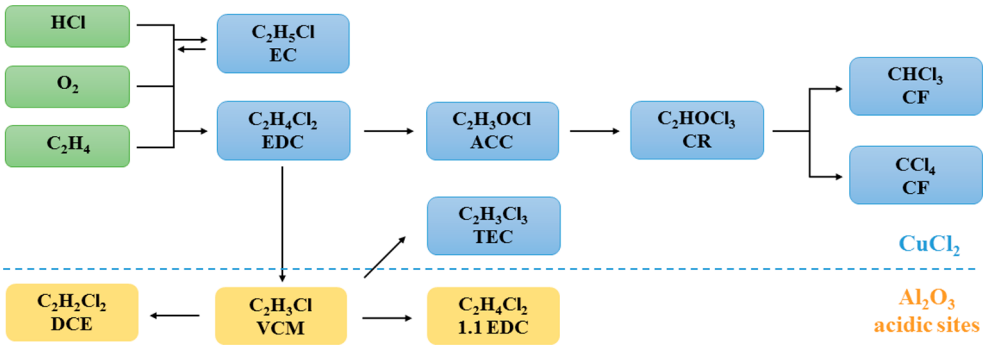

Figure 8. Catalyst functionality and reaction pathways of different organochlorine products in ethylene oxychlorination.

of various additives on the density of Lewis and Brønsted acidic sites of the γ-Al_2O_3 support was investigated. CsCl and KCl eliminated all the surface Lewis acidity, and LiCl, $MgCl_2$, and $LaCl_3$ also suppressed it significantly. All the dopants except CsCl increased the strength of the Brønsted sites.[76] They concluded that Lewis and Brønsted acid sites on the Al_2O_3 surface were responsible for the conversion of EDC to chlorinated byproducts, such as VCM, 1,1-EDC, and 1,2-dichloroethene (DCE). HCl can chlorinate the Al_2O_3 surface, and the surface Cl on alumina will be involved in the byproduct formation. The selectivity toward chlorinated byproducts correlates directly with the density of Lewis acid sites at a temperature of 300 °C or higher, in the order Cu5.0 > La10.9Cu5.0 > Li0.9Cu5.0 > Mg1.9Cu5.0 > K3.1Cu5.0 ≈ Cs10.4Cu5.0.[77] At 230 °C, the content of byproduct is very low, typically lower than 0.01−0.02.

It is generally accepted that the acidic sites catalyze the EDC dehydrochlorination to VCM.[49,73,118,119,122] The EDC dehydrochlorination is a first-order to EDC and hindered by water[123] and HCl at high temperatures (about 240 °C).[114] Consistent with the work of Muddada et al.[76,77] it has been proposed that pure alumina or chlorinated alumina are most active for dehydrochlorination. Adding promoters significantly reduces the dehydrochlorination of EDC and EC. The following order of the dehydrochlorination has been suggested:[114]

$$\text{Pure } Al_2O_3 > CuCl_2/Al_2O_3 > MgCl_2/Al_2O_3 > KCl/Al_2O_3$$

Based on the above analysis, alkaline metal chloride-promoted $CuCl_2$ catalysts are superior from the viewpoint of increasing the selectivity. Mile et al.[118] investigated the reaction mechanism and kinetics of dehydrochlorination of 1,2-EDC on different catalysts by kinetic isotope techniques. They observed a positive kinetic isotope ratio k_H/k_D for the production of 1,2-EDC on the undoped catalysts, which suggested C−H bond breaking is the rate-determining step. The promoter additives shifted the RDS from C−H bond breaking on unpromoted catalysts to C−Cl bond breaking. Besides, they found that the 1,2-EDC dehydrochlorination reaction is a first-order reaction with an activation energy of 103 kJ mol^{-1} at 558 K, and the addition of promoters increased the activation energies in the order of LiCl > CsCl > NaCl > KCl ∼ RbCl.

1,1,2-Trichloroethane (TEC) by Oxychlorination of VCM. From a quantitative viewpoint, 1,1,2-trichloroethane (TEC) is the most crucial chloro-organic admixture, and it accounts for about 35−40% total chloro-organic byproducts.[114] Muddada et al.[77] proposed that TEC was formed from EDC via VCM on Cu catalysts. $CuCl_2$ is more active than CuCl for the further reaction of VCM, and the reaction mechanism is similar to the ethylene oxychlorination where lattice Cl in $CuCl_2$ is involved in the reaction. It was suggested that the reaction is preferred to be operated at the reduction-favorable conditions to reduce the $CuCl_2$ concentration to inhibit the TEC formation. However, the CuCl concentration should be controlled at the conditions with compromise of the selectivity and stability. Moreover, it should be noted that the VCM is the key intermediate for the TEC formation, and acidic sites are required. Suppressing VCM formation is a preferred way to suppress the formation of TEC. The copromoter (K1.55La5.45Cu5.0) increased the activity of the Cu phase with moderate $CuCl_2$ concentration and decreased the acid sites on the alumina surface. Besides the promotion, the Cu loading is also an important parameter to reduce the TEC formation. By increasing Cu loading at a level up to a nominally complete "monolayer" coverage and poisoning the alumina surface nucleophilic sites, the activity increases due to the increased density of active sites, while EDC selectivity increases due to decreasing acidic sites.[67] In addition to modifying the catalyst, the reaction temperature is another parameter to tune the selectivity. The TEC yield increased exponentially with increasing the temperature.[123]

Chloral, Chloroform, and Carbon Tetrachloride. These compounds are another group of important chloro organic admixtures. Their total content in crude 1,2-dichloroethane is usually 0.3−0.4%. It was shown that chloral is a product of the partial oxidation of EDC to an intermediate of chloroacetaldehyde following an oxychlorination reaction on Cu catalysts as

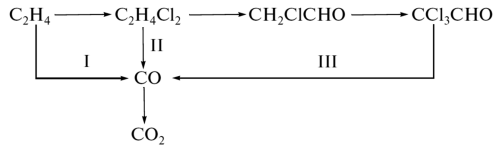

Figure 9. Reaction pathways for CO and CO_2 formation.

shown in Figure 9.[124] Decomposition of chloral forms chloroform, according to the reaction

$$C_2HOCl_3 \rightarrow CHCl_3 + CO \quad (11)$$

Carbon tetrachloride is formed via a chloral oxychlorination:

$$C_2HOCl_3 + HCl + 1/2O_2 \rightarrow CCl_4 + CO + H_2O \quad (12)$$

The reaction mechanism of the oxychlorination can be similar to the ethylene oxychlorination on $CuCl_2$ catalysts. The

https://dx.doi.org/10.1021/acscatal.0c01698
ACS Catal. 2020, 10, 9299−9319

ratio between the chloral decomposition and oxychlorination rates can be estimated at approximately 2:1 at low temperatures (210−215 °C).[114,124]

CO_x (CO and CO_2) is another group of byproducts which influences the product cost in industrial oxychlorination. There have several kinetic studies of the CO_x formation in oxychlorination mostly in the 1970s.[115] Three precursors for CO_x formation were identified.

The ratio between the rates of paths I, II, and III is approximately 1:2:0.3.[114] Ethylene oxychlorination and oxidation occur on the same active sites, and two reactions compete on the surface. At low temperatures, the oxychlorination is the dominating reaction, while at temperatures higher than 300 °C, the deep oxidation increased significantly. The mechanism of EDC oxidation can be rather different from the ethylene oxidation, which is presented in Figure 10.

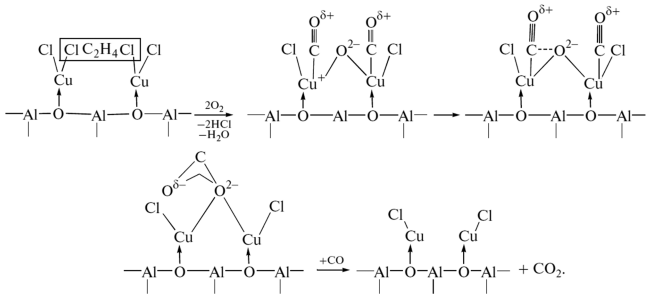

Figure 10. Mechanism of CO and CO_2 formation from EDC. Reproduced with permission from ref 115. Copyright 2015 Springer.

CuCl and Cu_2OCl_2 were suggested to be responsible for the CO_x formation. The O in Cu_2OCl_2 assisted the C−C bond cleavage. At the high conversion of HCl, the oxidation of ethylene and EDC was well described by the simple kinetic model with a reaction order of 1 to ethylene or EDC and a reaction order of 0.5 to oxygen. The apparent activation energy is 105 kJ/mol for EDC oxidation and 80.5 kJ/mol for ethylene oxidation, respectively. Higher temperature favors EDC oxidation to CO_x.

At the standard low-temperature oxychlorination process in the fixed-bed reactor, the ratio between the oxidation rates of EDC and ethylene is nearly 2:1. Higher temperatures (230−255 °C) typically used in the fluidized bed reactor favor the contribution from EDC oxidation to the formation of carbon oxides. At low conversions, the formation of carbon oxides is suppressed by HCl. This is the reason why the industrial operation is always at a little HCl excess to avoid the CO_x formation.

CO is the primary product of oxidation, and CO_2 is the secondary product of CO oxidation. The CuCl is responsible for the adsorption of CO and reacts with adjunct O in Cu_2OCl_2. The catalyst used in the ethylene oxychlorination process must also be active in the reaction of CO oxidation to CO_2. The selectivity to target EDC is positively related to the CO_2 content in the gas phase. It was found that the optimum CO_2/CO ratio in the products of the "air" flow process must be larger than 2:1 mol/mol. The ratio of CO_2/CO is one indicator of the process regime. A drop in this ratio close to and less than 2 indicates a lack of oxygen in the system. This disrupts the reduction and oxidation balance leading to CuCl dominating on the surface by slowing the CuCl reoxidation rate, thus deactivating the catalysts and degrading the quality of the fluidization of the catalysts. The operation using the concentrated oxygen is better than the air. The CO_2 to CO ratio can be a result of the following reaction:

$$\mathrm{ClCu{-}O{-}CuCl + CO \leftrightarrow ClCu{-}\square{-}CuCl + CO_2} \quad (13)$$

Assuming the reaction is close to equilibrium, the ratio of CO_2/CO can be described as

$$\frac{CO_2}{CO} = \frac{Cu^{2+}}{KCu^{+}} \sim \frac{[O]}{KCu^{+}} \quad (14)$$

The ratio of CO_2/CO reflects the ratio of $CuCl_2$/CuCl and surface [O] at the reaction conditions. As discussed above, the higher concentration of $CuCl_2$ is important to achieve high activity and stability of the oxychlorination catalysts, in addition to high selectivity to EDC.

As we discussed above in the section of active sites and promoter effect, the promoters can be effectively used to tune the $CuCl_2$/CuCl ratio in the reaction. The alkaline metal chloride as the promoter can effectively increase the $CuCl_2$ concentration under working conditions. Based on the above discussion, adding alkaline metal chlorides into Cu catalysts can suppress CO_x formation by increasing the $CuCl_2$/CuCl ratio. The hypothesis is confirmed by Arcoya et al. in ethylene oxychlorination on promoted $CuCl_2/\alpha$-Al_2O_3 where the CO and CO_2 selectivity follows an order of Cu > Cu−K > Cu−Na > Cu−La. The CO_x selectivity decreased from 5.2% on Cu to 0.6% on Cu−K, while adding the second promoters (Ce, Nd, Pr) into Cu−K catalysts, the CO_x selectivity reduced further to 0.1%.[49]

The effect of alkaline- and rare-earth metal chloride promoters on the CO and CO_2 selectivity is further examined by combining the tendency of $CuCl_2$ and the CO_2/CO ratio under working conditions. Table 4 summarized the CO and CO_2 mole fraction in ethylene oxychlorination on promoted $CuCl_2/\gamma$-Al_2O_3 at 498 K and C_2H_4:O_2:HCl = 1:1.8:0.9.[57]

Table 4. Effect of Promoters on the EDC Selectivity and CO and CO_2 Model Fraction in the Gas Phase as well as the $CuCl_2$/CuCl Ratio in Ethylene Oxychlorination

cat	Cu1.2La	Cu	CuK1.2La	CuK
EDC%[a]	97.0	96.9	97.5	97.8
CO%[b]	1.3	2.3	0.7	0.5
CO_2%[b]	2.4	5.2	2.1	1.7
(CO+CO_2) %	3.7	7.5	2.8	2.2
CO_2/CO	1.84	2.3	3	3.4
$CuCl_2$/CuCl[c]	+	++	+++	++++

[a]Ethylene dichloride selectivity. [b]Mole fraction in gas phase.[57] [c]The ratio was measured by UV−vis spectroscopy.[68]

In general, adding promoters to $CuCl_2$ reduced CO_x formation as shown in Table 4.[57] The $CuCl_2$ concentration or $CuCl_2$/CuCl at the steady state was measured by UV−vis spectroscopy.[68] Although the catalyst and the reaction conditions are not the same, the tendency of the $CuCl_2$/CuCl is expected to be similar. The catalysts with higher $CuCl_2$/CuCl resulted in a higher CO_2/CO ratio, especially for K and La−K copromoted catalysts. It is confirmed with the hypothesis of the CO_2/CO ratio as an indicator of $CuCl_2$/CuCl at the reaction conditions. Lower CuCl yielded a lower CO_x selectivity and higher selectivity to EDC. Muddada et al.[77] demonstrated that CO_2 can be also formed in EDC converting on alumina, and O on the alumina surface contributed to the

https://dx.doi.org/10.1021/acscatal.0c01698
ACS Catal. 2020, 10, 9299−9319

Table 5. Reaction Rate Expressions for Ethylene Oxychlorination

	catalyst	T (K)	equation	reaction order C_2H_4	reaction order O_2	reaction order HCl	reaction order H_2O	activation energy (kJ/mol)	ref
1	$CuCl_2/\gamma$-Al_2O_3	454−469	$r = 2.49 \times 10^{-6} \times (C_2H_4)^{0.73}(O_2)^{0.34}(H_2O)^{-0.18}$	0.73	0.34	0	−0.18	102.6	66
2	KCl+$CuCl_2$/silica	473−573	$r = kP^m_{C_2H_4}P^n_{HCl}P^l_{O_2}P^x_{H_2O}$	0.6	0.5	0.2	0		16
3	$CuCl_2$/charcoal			1	0	0.2	0		
4	$CuCl_2/\gamma$-Al_2O_3			1	1	0.3	0		
5	$CuCl_2/\gamma$-Al_2O_3 commercial	473−553	$r = kE^{-E_a/(R\Delta T)}P^{0.67}_{C_2H_4}$	0.67	0	0	0		126
6	$CuCl_2/\gamma$-Al_2O_3 commercial	483−523	$r = 1.21 \times 10^5 E^{-12300/(RT)}P^{1.61}_{C_2H_4}$	1.61	0	0	0	51.5	127
7	$CuCl_2/\gamma$-Al_2O_3	484−524	$r = 1.2127 \times 10^9 E^{-94671/(RT)}P^{1.61}_{C_2H_4}P^{0.25}_{O_2}$	1.61	0.25	0	0	94.7	128

Table 6. Reaction Rate Expressions for Ethylene Oxychlorination

	catalyst	T (K)	equation	activation energy (kJ/mol)	ref
1	$CuCl_2/\gamma$-Al_2O_3	457	$r = \frac{6.83 * 10^{-7}(C_2H_4)(O_2)^{0.5}}{[1 + 0.0017(C_2H_4) + 0.0355(O_2)^{0.5} + 0.0165(H_2O)]^2}$	102.5 (454−469 K)	66
2	$CuCl_2/\gamma$-Al_2O_3	473−553	$r_{EDC} = \frac{K_1'K_1''k_2P^2_{HCl}P_{C_2H_4}}{1 + K_1'P_{HCl}\left[1 + K_5 + K_1''P_{HCl}\left(1 + \frac{k_2P_{C_2H_4}}{k_3P_{O_2}}\right)\right]}$		129
3	$CuCl_2/\gamma$-Al_2O_3	423−523	$r = \frac{269e^{-37.8/RT}C_{C_2H_4}C_{CuCl_2}}{1 + 0.63C_{C_2H_4}}$ (Reduction step)	37.8	130
4	$CuCl_2/\gamma$-Al_2O_3	473−533	$r = k_1P_{C_2H_4}P^n_{O_2}\frac{P_{HCl}}{(1 + K_1P_{HCl})^2}$	111.5	131

reaction. However, the contribution to CO_x formation is much lower than on Cu catalyzed CO and CO_2 formation.

5. KINETICS FOR THE MAIN AND BYPRODUCT FORMATION

5.1. Kinetics on the EDC Formation. A deep understanding from the molecular level on the kinetics and the determination of structure−activity relationships has the fundamental meaning in the development of the heterogeneously catalyzed process. This knowledge is limited in ethylene oxychlorination, because of the demanding experimental conditions involving corrosive, toxic, and flammable reactant gases, which make it quite difficult to use the commonly used technique and setups to tackle the mechanistic investigations,[1] due to the significant industrial impact of ethylene oxychlorination. The studies that have been reported in the literature about the kinetics of ethylene oxychlorination are fewer than the studies that have been reported the other catalytic reactions. The first kinetic study of ethylene oxychlorination was carried out on the $CuCl_2/\gamma$-Al_2O_3 catalyst at the temperature of 473−573 K.[125] It was observed that the reaction rate of ethylene conversion is irrelated to the partial pressure of C_2H_4 but does depend on the partial pressure of O_2; what is more, the reaction is inhibited by EDC and HCl.

$$r = \frac{kP_{O_2}}{\{1 + AP_{C_2H_4Cl_2}/P_{O_2} + BP_{HCl} \times P_{O_2}\}^2} \quad (15)$$

The kinetic model suggests the reaction is fully controlled by the CuCl oxidation. Afterward, a great deal of effort has been devoted to the study of the kinetics of the main reaction. The simple power-law model was widely used to correlate the reaction rate and the process variables. It has also proved the very good fitting with analogous experimental results, and the conclusions are summarized in Table 5.

Some rate equations based on the Langmuir−Hinshelwood-Hougen-Waston type were also proposed and summarized in Table 6.

The reported kinetics varies very much. In general, the reaction order for ethylene and HCl is close to 1 and 0, respectively. It is in good agreement with the observation that hydrochlorination is fast and kinetically irrelevant. Thus, the reaction rate is independent of HCl pressure. However, the reaction order to oxygen varied very much between 0 to 1. For the commercial catalysts which are typically promoted by promoters, the reaction order to oxygen is about zero, which possibly pointed out the $CuCl_2$ reduction by ethylene is the rate-determining step, which is consistent with the experimental observation for K-promoted catalysts as discussed above.[35,36] The kinetics is also related to the catalyst support.[16] It suggests that the support can change the properties of $CuCl_2$ catalyst properties, and especially the oxidation of CuCl, which lies well above the discussion of the support effect. It seems that the charcoal facilitates the oxygen activation and CuCl oxidation, leading to a zero-order to oxygen. On some catalysts, the reaction order to oxygen is 1, suggesting adsorption and dissociation of oxygen could become the RDS. Moreover, most of the apparent activation energy on $CuCl_2/\gamma$-Al_2O_3 is in the range of 94.7−111.5 kJ/mol. The activation energy for the step of the $CuCl_2$ reduction step by ethylene was measured to be 37.8 kJ/mol.[130] The value is similar to the one (51.5 kJ/mol) for the reaction with reduction as the RDS on the commercial catalysts most likely K-promoted.[127] Therefore, the kinetics depends significantly on catalyst properties, such as different supports and promoters.

5.2. Kinetics on Byproduct Formation. As known, the selectivity determines the technology and finally affects the economic efficiency of the process. CO_x is one of the important byproducts formed by deep oxidation from ethylene and EDC in ethylene oxychlorination. It was first established

https://dx.doi.org/10.1021/acscatal.0c01698
ACS Catal. 2020, 10, 9299−9319

that the rate of the deep oxidation reaction increased along with the O_2 and C_2H_4 partial pressures and slows upon an increase in the HCl partial pressure.[115] The rate of the ethylene and EDC oxidation reaction can be written in a general form as[114]

$$r_{CO_x} = \frac{kC_iC_{O_2}}{1 + k_1C_{O_2} + K_2C_{HCl}} \quad (16)$$

where C_i is the concentration of ethylene or EDC. It is noted that when a catalyst is highly active in the target ethylene oxychlorination reaction (the HCl conversion exceeds 99%), the above equation can be simplified as

$$r_{CO_x} = \frac{kC_iC_{O_2}}{1 + k_1C_{O_2}} \quad (17)$$

The Arrhenius parameters of C_2H_4 and EDC oxidation reactions within the temperature range of 215−235 °C are expressed as

$$k_{EDC} = 5.6 \times 10^9 \exp[-105000/RT] \quad (18)$$

$$k_{C_2H_4} = 6.3 \times 10^6 \exp[-80500/RT] \quad (19)$$

It can be easily calculated that at the standard reaction temperature of the ethylene oxychlorination process, the ratio between the rates of EDC and C_2H_4 oxidation is nearly 2:1. Higher temperatures (230−255 °C) favor an increase in the contribution from EDC oxidation to the formation of CO_2.

Another type of byproduct is the organochlorine products contain chlorine-substituted C_1−C_2 paraffin and olefins, along with some O_2-containing chlorinated hydrocarbons.[114] Herein, we will choose a part to show the kinetic study on the byproduct formation.

Ethyl chloride (C_2H_5Cl) is formed by the ethylene hydrochlorination reaction. It occurs according to an equation of first-order with respect to C_2H_4 and HCl and is inhibited by water vapor, following the equation of

$$r_{C_2H_5Cl} = \frac{kP_{C_2H_4}P_{HCl}}{1 + K_{H_2O}P_{H_2O}} \quad (20)$$

The equation suggests that the selectivity of ethyl chloride can be minimized by using water vapor as a fluidizing agent instead of N_2 in the air process or a recycled gas in the O_2 process.

Another important byproduct is VCM (C_2H_3Cl), formed by dehydrochlorination of EDC. It was reported that the rate of vinyl chloride formation at a relatively lower temperature (200−215 °C) can be described by the first-order equation

$$r_{VCM} = kP_{EDC} \quad (21)$$

When the temperature is raised to 240 °C, some deviation from the linear relationship is observed, probably due to the inhibition by HCl, which is also one of the products. The rate of the reaction can be formulated in a general form of

$$r_{VCM} = \frac{kP_{EDC}}{1 + k_1P_{HCl}} \quad (22)$$

To sum up, we have summarized the kinetic study on ethylene oxychlorination on both the product of EDC and several main byproducts, as summarized in Figure 11. It is noteworthy that it is a very complex catalytic reaction involving a number of reactions, like oxychlorination, hydrochlorination,

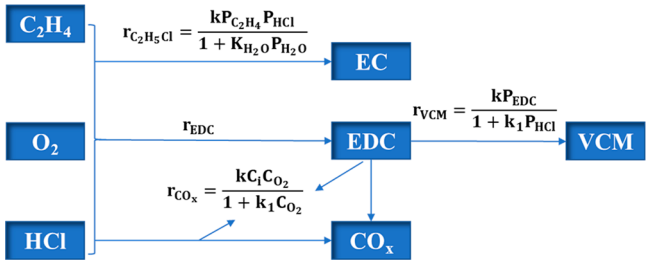

Figure 11. Kinetic expressions on the product and main byproducts. (Herein the expression of r_{EDC} can be found in Tables 5 and 6.)

deep oxidation, dehydrochlorination, etc. Enrico and co-workers[131] developed a new kinetic model for the ethylene oxychlorination reaction network including nine chemical reactions to describe the evolution of 12 species (including six major byproducts) based on 28 kinetic runs performed over a commercial $CuCl_2/\gamma$-Al_2O_3 catalyst in a dedicated tubular flow reactor. The main byproducts are ethyl chloride (C_2H_5Cl), 1,1,2-trichloroethane ($C_2H_3Cl_3$), chloral (C_2Cl_3HO), carbon tetrachloride (CCl_4), chloroform ($CHCl_3$), CO, and CO_2.

Although numerous studies have been devoted to the kinetic study in ethylene oxychlorination over the $CuCl_2/Al_2O_3$-based catalyst, many possible and potential correlations remain open and need to be studied further.

6. CONCLUSIONS AND PERSPECTIVE

The balanced VCM process is still the leading-edge technology for PVC production in the world, where ethylene oxychlorination plays a key role in the process. Although the $CuCl_2$-based catalysts with proper promoters have been commonly used as the industrial catalyst for several decades, formidable challenges remain to be solved regarding the design of more efficient catalysts suppressing Cu volatilization and agglomeration to make more stable catalysts as well as reducing the byproduct formation. Here, the in-depth analysis of the fundamental understanding of the reaction mechanism, ethylene oxychlorination chemistry, materials, and active sites including the interaction of $CuCl_2$ with support and promoters has been conducted.

The yield of products depends on the catalyst properties, feedstocks, reaction conditions, and reactor types such as a fixed-bed or fluidized bed reactor. In the catalytic cycle, three steps are involved: in the reduction step, $CuCl_2$ is reduced by ethylene with EDC formed; in the oxidation step, CuCl is oxidized by O_2 to Cu_2OCl_2; in the hydrochlorination step, the Cu_2OCl_2 is recovered to $CuCl_2$ by HCl. The lattice Cl vacancy will be filled by oxygen once Cl was removed from $CuCl_2$ by attacking of ethylene. At the steady-state operation, the catalyst reduction and oxidation are kinetically balanced to hold the certain distribution of $CuCl_2$ and Cl vacancy, and the combined $CuCl_2$ and Cl vacancy is the active site. Different from the conventional heterogeneous catalysts, the active sites are highly dynamic, depending on the local chemical atmosphere such as concentrations and temperatures through the kinetic balance. The composition of the active sites is the key to control the activity, selectivity, and stability. The catalyst should be designed to keep as high as possible the $CuCl_2$ and less Cl vacancy to suppress the Cu loss due to the high volatility of CuCl and reduce the CO_x formation catalyzed by CuCl. The rate-diagram is a powerful tool to predict the reaction rate and $CuCl_2$ concentration at the steady state and

https://dx.doi.org/10.1021/acscatal.0c01698
ACS Catal. 2020, 10, 9299−9319

to guide tuning the reduction and oxidation rate to achieve better catalysts. The reduction and oxidation properties of the catalyst can be modified by the catalyst supports and the promoters. The epitaxial growth of the $CuCl_2$ layer on the supports results in a significant support dependence of the support. New catalyst supports should be explored to manipulate the $CuCl_2$ properties. γ-Al_2O_3 is the most commonly used support for an industrial $CuCl_2$ catalyst, and the properties of γ-Al_2O_3 can be optimized in terms of exposure of facets such as (111), (100), and (110).

Certain promoters (like K and Cs) can form a complex with $CuCl_2$ on the support surface, playing a significant role in improving the catalytic performance, which is why we dedicated the majority of this Review to their delineation. The promoter can be categorized into two classes: one leading to a relatively low reaction rate but high $CuCl_2$, thus good stability of oxychlorination catalyst; one enhances both $CuCl_2$ reduction and the CuCl oxidation, leading to a high reaction rate but mediate $CuCl_2$ concentration. Adding promoters can increase the fraction of the active Cu species, due to the ability of the corresponding cations to compete with $CuCl_2$ filling in the vacancies of Al_2O_3. Continued efforts should be put on the promoter effect in this industrial reaction to further increase the fraction of the active Cu species by enhancing the oxidation of CuCl. Bi- or multipromoters can be designed to enhance the activity, selectivity, and stability. There is a large family expected that can be combined to tune the reduction, oxidation, and hydrochlorination activity, thus compromising the activity and stability at the steady state. More fundamental studies are highly required to understand the interaction of multipromoters with $CuCl_2$ and gain a better principle for catalyst design to achieve better performance.

Additionally, the process intensification occurs by integrating the current two-step (ethylene oxychlorination to form EDC and EDC dehydrochlorination to produce VCM) into one single step. However, only a few results were reported so far, since the operating conditions vary a great deal for the two reactions (oxychlorination-dehydrochlorination) as we discussed above. The $CuCl_2$-based catalyst, commonly used in the industry for ethylene oxychlorination nowadays, cannot meet the requirement for dehydrochlorination at higher temperatures, at which the volatilization of CuCl becomes remarkable, which will further cause the deactivation. Therefore, more efforts can be focused on developing the bifunctional catalysts, which can catalyze the ethylene oxychlorination and EDC dehydrochlorination simultaneously with high energy efficiency. Another process we can put more attention towards is utilizing the ethane oxychlorination to directly produce VCM. Ethane obtained from natural gas is cheap and is almost an inexhaustible resource for the petrochemical industry. Developing an ethane-based technology would be a breakthrough for VCM manufacturing in the future. However, despite its great potential, an ethane-based technology is still under exploration. More efforts can be made to develop better catalysts making this process more efficient.

Catalyst development relies on a better fundamental understanding of the process. It would benefit significantly from the *in situ* characterization techniques to monitor structure and active site evolution under working conditions, as well as advanced computational tools to further explore reaction dynamics. Detailed kinetic modeling coupling with DFT calculation of the whole catalytic cycle could help provide a deeper understanding of the catalysis and provide a predictive model for kinetics and rational catalyst design. More effort should be devoted to the kinetic study and modeling of the whole catalytic cycle and provide a detailed microkinetic model to predict not only the reaction rates of the formation of the products but also the active site evolution in the redox cycle in chemical reactors. Effective techniques to characterize alumina surface properties will be highly beneficial for controlling the alumina properties and guiding industrial production. Thus, academia should work together with industry to devote more to greatly accelerate the development of ethylene oxychlorination both fundamentally and commercially.

AUTHOR INFORMATION

Corresponding Authors

Kumar R. Rout − *Department of Chemical Engineering, Norwegian University of Science and Technology, N-7491 Trondheim, Norway; Sintef Industry, N-7491 Trondheim, Norway*; Email: kumarranjan.rout@sintef.no

De Chen − *Department of Chemical Engineering, Norwegian University of Science and Technology, N-7491 Trondheim, Norway*; orcid.org/0000-0002-5609-5825; Email: de.chen@ntnu.no

Authors

Hongfei Ma − *Department of Chemical Engineering, Norwegian University of Science and Technology, N-7491 Trondheim, Norway*

Yalan Wang − *Department of Chemical Engineering, Norwegian University of Science and Technology, N-7491 Trondheim, Norway*

Yanying Qi − *Department of Chemical Engineering, Norwegian University of Science and Technology, N-7491 Trondheim, Norway*

Complete contact information is available at: https://pubs.acs.org/10.1021/acscatal.0c01698

Author Contributions

[§]H.M., Y.W., and Y.Q. contributed equally.

Notes

The authors declare no competing financial interest.

ACKNOWLEDGMENTS

The authors greatly acknowledge the financial support from the center of industrial Catalysis Science and Innovation (iCSI), a center for Research-based Innovation funded by the Research Council of Norway (Grant No. 237922).

REFERENCES

(1) Lin, R.; Amrute, A. P.; Perez-Ramirez, J. Halogen-Mediated Conversion of Hydrocarbons to Commodities. *Chem. Rev.* **2017**, *117*, 4182−4247.

(2) Davies, C. J.; Miedziak, P. J.; Brett, G. L.; Hutchings, G. J. Vinyl Chloride Monomer Production Catalysed by Gold: A Review. *Chin. J. Catal* **2016**, *37*, 1600−1607.

(3) Global Production Capacity of Vinyl Chloride Monomer 2018 & 2023. Published by M. Garside. https://www.statista.com/statistics/1063677/global-vinyl-chloride-monomer-production-capacity/ (accessed 2019-11-06).

(4) Hutchings, G. J.; Kiely, C. J. Strategies for the Synthesis of Supported Gold Palladium Nanoparticles with Controlled Morphology and Composition. *Acc. Chem. Res.* **2013**, *46*, 1759−1772.

(5) Xu, H.; Luo, G. H. Green Production of PVC From Laboratory to Industrialization: State-of-the-art Review of Heterogeneous Non-

Mercury Catalysts for Acetylene Hydrochlorination. *J. Ind. Eng. Chem.* **2018**, *65*, 13−25.
(6) Chemmangattuvalappil, N. G.; Chon, C. H.; Sum, D. N. K.; Elyas, R.; Chen, C.-L.; Chien, I. L.; Lee, H.-Y.; Elms, R. D. *Chemical Engineering Process Simulation*; Elsevier: 2017.
(7) Kurta, S.; Mykytyn, I.; Khatsevich, O.; Ribun, V. Mechanism of Catalytic Additive Chlorination of Ethylene to 1, 2-Dichloroethane. *Theor. Exp. Chem.* **2018**, *54*, 283−291.
(8) Galitzenstein, E.; Woolf, C. The Chlorination of Ethylene and Propylene. I. The Chlorination of Ethylene. *J. Soc. Chem. Ind., London* **1950**, *69*, 289−292.
(9) Severino, F. T. Process for Chlorination of Ethylene. US Patent, US4172099A, 1979.
(10) Naworski, J.; Velez, E. i. Oxychlorination of Ethylene. *Applied Industrial Catalysis*; Elsevier: 1983; pp 239−273.
(11) Magistro, A. J.; Cowfer, J. A. Oxychlorination of Ethylene. *J. Chem. Educ.* **1986**, *63*, 1056−1058.
(12) Dimian, A. C.; Bildea, C. S. *Chemical Process Design: Computer-aided Case Studies*; John Wiley & Sons: 2008; DOI: 10.1002/9783527621583.
(13) Wilkes, C. E.; Summers, J. W.; Daniels, C. A.; Berard, M. T. *PVC handbook*; Hanser: Munich, 2005.
(14) Hall, P. G.; Heaton, P.; Rosseinsky, D. R. Adsorption and Conductivity Studies in Oxychlorination Catalysis. Part 3. The Ethene Transition-metal Chloride Interaction. *J. Chem. Soc., Faraday Trans. 1* **1984**, *80*, 3059−3070.
(15) Agnew, J.; Shankar, H. Catalyst Deactivation in Acetylene Hydrochlorination. *Ind. Eng. Chem. Prod. Res. Dev.* **1986**, *25*, 19−22.
(16) Treger, Y. A.; Rozanov, V. N.; Flid, M. R.; Kartashov, L. M. Oxidative Chlorination of Aliphatic Hydrocarbons and Their Chloro-derivatives. *Russ. Chem. Rev.* **1988**, *57*, 326.
(17) Hickman, D. A.; Jones, M. E.; Jovanovic, Z. R.; Olken, M. M.; Podkolzin, S. G.; Stangland, E. E.; Thompson, R. K. Reactor Scale-up for Fluidized Bed Conversion of Ethane to Vinyl Chloride. *Ind. Eng. Chem. Res.* **2010**, *49*, 10674−10681.
(18) Blanco, J.; Fayos, J.; De La Banda, J. G.; Soria, J. Study of Supported Copper Chloride Catalysts by Electron Paramagnetic Resonance and X-Ray Diffraction. *J. Catal.* **1973**, *31*, 257−263.
(19) Boulamanti, A.; Moya, J. *Energy efficiency and GHG emissions: Prospective scenarios for the Chemical and Petrochemical Industry*; Publications Office of the European Union: 2017; DOI: 10.2760/630308.
(20) Mallikarjunan, M.; Hussain, S. Z. Oxychlorination of Some Lower Aliphatic Hydrocarbons. *J. Sci. Ind. Res.* **1983**, *42*, 209−229.
(21) Todo, N.; Hagiwara, H.; Kurita, M. Catalysts for Oxy-chlorination Reaction. The correlation between Deacon process and oxychlo-rination. *Kogyo Kagaku Zasshi* **1966**, *69*, 1463−1466.
(22) Allen, J.; Clark, A. Oxychlorination catalysts. *Rev. Pure Appl. Chem.* **1971**, *21*, 145−166.
(23) Allen, J. Energetic Criteria for Oxychlorination Catalysts. *J. Appl. Chem.* **1962**, *12*, 406−412.
(24) Muddada, N. B. The Influence of Dopants on Copper Chloride Catalysts for Ethylene Oxychlorination Reaction. Doctoral Thesis, University of Oslo, Norway, 2013.
(25) Dugan, J. J. Catalyst System. US Patent, US3670037A, 1972.
(26) Wakiyama, S.; Uchida, K. Process for Oxychlorination of Ethylene. US Patent, US3624170, 1971.
(27) Magistro, Aj; Nicholas, P. P.; Carroll, R. T. Oxychlorination of Ethylene at High Temperatures. *J. Org. Chem.* **1969**, *34*, 271−273.
(28) Lemanski, M. F.; Leitert, F. C.; Vinson, C. G., Jr. Catalyst and Process for Production of VCM. US Patent, US4115323, 1978.
(29) Born, J.; De Lijser, H.; Ahonkhai, S.; Louw, R.; Mulder, P. Fly Ash Mediated Oxychlorination and Oxidation of Ethylene. *Chemosphere* **1991**, *23*, 1213−1220.
(30) Scharfe, M.; Lira-Parada, P. A.; Paunovic, V.; Moser, M.; Amrute, A. P.; Perez-Ramirez, J. Oxychlorination-Dehydrochlorination Chemistry on Bifunctional Ceria Catalysts for Intensified Vinyl Chloride Production. *Angew. Chem., Int. Ed.* **2016**, *55*, 3068−3072.
(31) Higham, M. D.; Scharfe, M.; Capdevila-Cortada, M.; Perez-Ramirez, J.; Lopez, N. Mechanism of Ethylene Oxychlorination over Ruthenium Oxide. *J. Catal.* **2017**, *353*, 171−180.
(32) Jones, M. E.; Olken, M. M.; Hickman, D. A. Process for the Conversion of Ethylene to Vinyl Chloride and Novel Catalyst Compositions Useful for Such Process. US Patent, US6909024B1, 2005.
(33) Scharfe, M.; Lira-Parada, P. A.; Amrute, A. P.; Mitchell, S.; Perez-Ramirez, J. Lanthanide Compounds as Catalysts for the One-Step Synthesis of Vinyl Chloride from Ethylene. *J. Catal.* **2016**, *344*, 524−534.
(34) Scharfe, M.; Capdevila-Cortada, M.; Kondratenko, V. A.; Kondratenko, E. V.; Colussi, S.; Trovarelli, A.; Lopez, N.; Perez-Ramirez, J. Mechanism of Ethylene Oxychlorination on Ceria. *ACS Catal.* **2018**, *8*, 2651−2663.
(35) Gianolio, D.; Muddada, N. B.; Olsbye, U.; Lamberti, C. Doped-$CuCl_2/Al_2O_3$ Catalysts for Ethylene Oxychlorination: Influence of Additives on the Nature of Active Phase and Reducibility. *Nucl. Instrum. Methods Phys. Res., Sect. B* **2012**, *284*, 53−57.
(36) Lamberti, C.; Prestipino, C.; Bonino, F.; Capello, L.; Bordiga, S.; Spoto, G.; Zecchina, A.; Moreno, S. D.; Cremaschi, B.; Garilli, M.; Marsella, A.; Carmello, D.; Vidotto, S.; Leofanti, G. The Chemistry of the Oxychlorination Catalyst: an in situ, Time-resolved XANES Study. *Angew. Chem., Int. Ed.* **2002**, *41*, 2341−2344.
(37) Leofanti, G.; Padovan, M.; Garilli, M.; Carmello, D.; Marra, G. L.; Zecchina, A.; Spoto, G.; Bordiga, S.; Lamberti, C. Alumina-supported Copper Chloride 2. Effect of Aging and Thermal Treatments. *J. Catal.* **2000**, *189*, 105−116.
(38) Leofanti, G.; Padovan, M.; Garilli, M.; Carmello, D.; Zecchina, A.; Spoto, G.; Bordiga, S.; Palomino, G. T.; Lamberti, C. Alumina-supported Copper Chloride 1. Characterization of Freshly Prepared Catalyst. *J. Catal.* **2000**, *189*, 91−104.
(39) Louwerse, M. J.; Rothenberg, G. Modeling Catalyst Preparation: The Structure of Impregnated−Dried Copper Chloride on γ-Alumina at Low Loadings. *ACS Catal.* **2013**, *3*, 1545−1554.
(40) Muddada, N. B.; Olsbye, U.; Caccialupi, L.; Cavani, F.; Leofanti, G.; Gianolio, D.; Bordiga, S.; Lamberti, C. Influence of Additives in Defining the Active Phase of The Ethylene Oxychlorination Catalyst. *Phys. Chem. Chem. Phys.* **2010**, *12*, 5605−5618.
(41) Garcia, C. L.; Resasco, D. E. Effects of the Support and The Addition of a Second Promoter on Potassium Chloride-Copper (II) Chloride Catalysts Used in the Oxychlorination of Methane. *Appl. Catal.* **1989**, *46*, 251−267.
(42) Leofanti, G.; Marsella, A.; Cremaschi, B.; Garilli, M.; Zecchina, A.; Spoto, G.; Bordiga, S.; Fisicaro, P.; Prestipino, C.; Villain, F.; Lamberti, C. Alumina-supported Copper Chloride - 4. Effect of Exposure to O_2 and HCl. *J. Catal.* **2002**, *205*, 375−381.
(43) Neurock, M.; Zhang, X. Y.; Olken, M.; Jones, M.; Hickman, D.; Calverley, T.; Gulotty, R. A First-Principle Analysis of Ethylene Chemisorption on Copper Chloride Clusters. *J. Phys. Chem. B* **2001**, *105*, 1562−1572.
(44) Qi, Y.; Fenes, E.; Ma, H.; Wang, Y.; Rout, K. R.; Fuglerud, T.; Piccinini, M.; Chen, D. Origin of Potassium Promotion Effects on $CuCl_2/\gamma$-Al_2O_3 Catalyzed Ethylene Oxychlorination. *Appl. Surf. Sci.* **2020**, *521*, 146310.
(45) Qi, Y.; Fenes, E.; Ma, H.; Wang, Y.; Rout, K. R.; Fuglerud, T.; Piccinini, M.; Chen, D. Cluster-Size-Dependent Interaction between Ethylene and $CuCl_2$ Clusters Supported via γ-Alumina. *J. Phys. Chem. C* **2020**, *124*, 10430−10440.
(46) Hammer, R. R.; Gregory, N. W. Vaporization Reactions in the Copper Chloride-Chlorine System. *J. Phys. Chem.* **1964**, *68*, 3229−3233.
(47) Rout, K. R.; Baidoo, M. F.; Fenes, E.; Zhu, J.; Fuglerud, T.; Chen, D. Understanding of Potassium Promoter Effects on Oxy-chlorination of Ethylene by Operando Spatial-time Resolved UV-vis-NIR Spectrometry. *J. Catal.* **2017**, *352*, 218−228.
(48) Rout, K. R.; Fenes, E.; Baidoo, M. F.; Abdollahi, R.; Fuglerud, T.; Chen, D. Highly Active and Stable CeO_2-Promoted $CuCl_2/Al_2O_3$

Oxychlorination Catalysts Developed by Rational Design Using a Rate Diagram of the Catalytic Cycle. *ACS Catal.* **2016**, *6*, 7030−7039.
(49) Arcoya, A.; Cortes, A.; Seoane, X. L. Optimization of Copper Chloride Based Catalysts for Ethylene Oxyhydrochlorination. *Can. J. Chem. Eng.* **1982**, *60*, 55−60.
(50) Rouco, A. TPR Study of Al_2O_3-and SiO_2-supported $CuCl_2$ Catalysts. *Appl. Catal., A* **1994**, *117*, 139−149.
(51) Lamberti, C.; Bordiga, S.; Bonino, F.; Prestipino, C.; Berlier, G.; Capello, L.; D'Acapito, F.; Xamena, F.; Zecchina, A. Determination of the Oxidation and Coordination State of Copper on Different Cu-based Catalysts by XANES Spectroscopy in situ or in Operando Conditions. *Phys. Chem. Chem. Phys.* **2003**, *5*, 4502−4509.
(52) Mallikarjunan, M. M.; Hussain, S. Z. Direct Oxychlorination of Ethylene to Vinyl-chloride Monomer. *J. Sci. Ind. Res.* **1984**, *43*, 94−97.
(53) Punnoose, A.; Seehra, M. S.; Dunn, B. C.; Eyring, E. M. Characterization of $CuCl_2/PdCl_2$/activated Carbon Catalysts for the Synthesis of Diethyl Carbonate. *Energy Fuels* **2002**, *16*, 182−188.
(54) GARCiA, C. L.; Resasco, D. E. High-temperature Oxychlorination Catalysts: Role of $LaCl_3$ as an Inhibitor of the Segregation of Active Species During Heating/cooling Cycles. *J. Catal.* **1990**, *122*, 151−165.
(55) Zipelli, C.; Bart, J.; Petrini, G.; Galvagno, S.; Cimino, C. Study of $CuCl_2$ Supported on SiO_2 and Al_2O_3. *Z. Anorg. Allg. Chem.* **1983**, *502*, 199−208.
(56) Wolf, F.; Kreissl, S.; Sonntag, O. Oxidation of Ethylene. *Chemische Technik* **1973**, *25*, 156−158.
(57) Rouco, A. J. Low-temperature Ethylene Oxyhydrochlorination: Effects of Supports and Promoters on The Mobilities of Active Species in $CuCl_2$ Catalysts. *J. Catal.* **1995**, *157*, 380−387.
(58) Fortini, E.; Garcia, C.; Resasco, D. Stabilization of the Active Phase by Interaction with the Support in $CuCl_2$ Oxychlorination Catalysts. *J. Catal.* **1986**, *99*, 12−18.
(59) Pieters, W. J. M.; Conner, W. C.; Carlson, E. J. The Oxyhydrochlorination of Methane on Fumed Silica-based Cu^{+1}, K, La Catalysts: I. Catalyst Synthesis. *Appl. Catal.* **1984**, *11*, 35−48.
(60) Dotson, R. L. Selected Properties and Electronic Spectra for A Series of Copper (II) Alkali, Alkaline Earth, and Lanthanide Metal Chloride Oxyhydrochlorination Catalysts on Alumina. *J. Catal.* **1974**, *33*, 210−218.
(61) Vajglova, Z.; Kumar, N.; Eranen, K.; Tokarev, A.; Peurla, M.; Peltonen, J.; Murzin, D. Y.; Salmi, T. Influence of the Support of Copper Catalysts on Activity and 1,2-Dichloroethane Selectivity in Ethylene Oxychlorination. *Appl. Catal., A* **2018**, *556*, 41−51.
(62) Stiles, A. B. *Catalyst Supports and Supported Catalysts*; Butterworth: Boston, 1987; Chapter 5.
(63) Deacon, H. Manufacture of Chlorine. US Patent, US85370, 1868.
(64) Deacon, H. Improvement in the Manufacture of Chlorine. US Patent, US118209, 1871.
(65) Ernst, O.; Wahl, H. D. E. Patent, 486952, 1929.
(66) Carrubba, R. V.; Spencer, J. L. Kinetics of Oxychlorination of Ethylene. *Ind. Eng. Chem. Process Des. Dev.* **1970**, *9*, 414−419.
(67) Leofanti, G.; Marsella, A.; Cremaschi, B.; Garilli, M.; Zecchina, A.; Spoto, G.; Bordiga, S.; Fisicaro, P.; Berlier, G.; Prestipino, C.; Casali, G.; Lamberti, C. Alumina-supported Copper Chloride 3. Effect of Exposure to Ethylene. *J. Catal.* **2001**, *202*, 279−295.
(68) Baidoo, M. F.; Fenes, E.; Rout, K. R.; Fuglerud, T.; Chen, D. On the Effects of K and La Co-promotion on $CuCl_2/\gamma$-Al_2O_3 Catalysts for the Oxychlorination of Ethylene. *Catal. Today* **2018**, *299*, 164−171.
(69) Weckhuysen, B. M. Determining the Active Site in A Catalytic Process: Operando Spectroscopy Is More Than A Buzzword. *Phys. Chem. Chem. Phys.* **2003**, *5*, 4351−4360.
(70) Loos, M.; Goulon, J.; Bertucci, M.; Bachelard, R. Structural Studies Using XAS of the Active Species Catalysing the Oxychlorination of Ethylene - II. *Phys. B* **1989**, *158*, 188−190.
(71) Prestipino, C.; Bordiga, S.; Lamberti, C.; Vidotto, S.; Garilli, M.; Cremaschi, B.; Marsella, A.; Leofanti, G.; Fisicaro, P.; Spoto, G. Structural Determination of Copper Species on the Alumina-Supported Copper Chloride Catalyst: A Detailed EXAFS Study. *J. Phys. Chem. B* **2003**, *107*, 5022−5030.
(72) Muddada, N. B.; Olsbye, U.; Leofanti, G.; Gianolio, D.; Bonino, F.; Bordiga, S.; Fuglerud, T.; Vidotto, S.; Marsella, A.; Lamberti, C. Quantification of Copper Phases, Their Reducibility and Dispersion in Doped-$Cucl_2/Al_2O_3$ Catalysts for Ethylene Oxychlorination. *Dalton Trans.* **2010**, *39*, 8437−8449.
(73) Finocchio, E.; Rossi, N.; Busca, G.; Padovan, M.; Leofanti, G.; Cremaschi, B.; Marsella, A.; Carmello, D. Characterization and Catalytic Activity of $CuCl_2$-Al_2O_3 Ethylene Oxychlorination Catalysts. *J. Catal.* **1998**, *179*, 606−618.
(74) Xie, Y.-C.; Tang, Y.-Q. Spontaneous Monolayer Dispersion of Oxides and Salts onto Surfaces of Supports: Applications to Heterogeneous Catalysis. *Advances in Catalysis*; Elsevier: 1990; Vol. *37*, pp 1−43, DOI: 10.1016/S0360-0564(08)60362-4.
(75) Xie, Y.; Zhang, H.; Wang, R. Kinetic Behaviour and Mechanism of Oxychlorination Catalyst. *Science China Mathematics* **1980**, *23*, 979−991.
(76) Muddada, N. B.; Olsbye, U.; Fuglerud, T.; Vidotto, S.; Marsella, A.; Bordiga, S.; Gianolio, D.; Leofanti, G.; Lamberti, C. The Role of Chlorine and Additives on the Density and Strength of Lewis and Bronsted Acidic Sites of gamma-Al_2O_3 Support Used in Oxychlorination Catalysis: A FTIR Study. *J. Catal.* **2011**, *284*, 236−246.
(77) Muddada, N. B.; Fuglerud, T.; Lamberti, C.; Olsbye, U. Tuning the Activity and Selectivity of $CuCl_2/\gamma$-Al_2O_3 Ethene Oxychlorination Catalyst by Selective Promotion. *Top. Catal.* **2014**, *57*, 741−756.
(78) Baidoo, M. F. Ethylene Oxychlorination on $CuCl_2$-based Oxychlorination Catalyst: Operando Kinetic Studies. Doctoral Thesis, Norwegian University of Science and Technology, Norway, 2019.
(79) Podkolzin, S. G.; Stangland, E. E.; Jones, M. E.; Peringer, E.; Lercher, J. A. Methyl Chloride Production from Methane over Lanthanum-based Catalysts. *J. Am. Chem. Soc.* **2007**, *129*, 2569−2576.
(80) Zhitao, C.; Minghan, H.; Dezheng, W.; Fei, W. Influence of Cerium on the Stability of Copper-based Oxychlorination Catalyst. *Chin. J. Catal.* **2008**, *29*, 951−953.
(81) Li, C.; Zhou, G. D.; Wang, L. P.; Li, Z.; Xue, Y. X.; Cheng, T. X. Effect of Impregnation Procedure of La_2O_3 Precursor on Copper-based Catalysts for Ethane Oxychlorination. *Catal. Commun.* **2011**, *13*, 22−25.
(82) Eden, J. S.; Cowfer, J. A. Catalyst and Process for the Fluid-bed Oxychlorination of Ethylene to EDC. US Patent, US4849393, 1989.
(83) Hirschmann, R. P.; Beard, W. O., Jr.; Mainz, E. L.; Smith, E. B.; Little, B. M. Oxychlorination Catalyst Compositions and Process of Making Same. US Patent, US5098878A 199, 1992.
(84) Mainz, E. L.; Beard, W. Q., Jr.; Hirschmann, R. P.; Little, B. M.; Smith, E. B. Oxychlorination Process Using a C.atalyst Which Comprises Copper Chloride Supported on Rare-Earth Modified Alumina. US Patent, US5113027A, 1992.
(85) Mainz, E. L.; Beard, W. Q., Jr.; Hirschmann, R. P.; Little, B. M.; Smith, E. B. Oxychlorination Catalysts Comprising Copper Chloride Supported on Rare-Earth-Modified Alumina, Process for Making Such Catalysts, and Oxychlorination Processes Using Them. US Patent, US5192733A, 1993.
(86) Carmello, D.; Fatutto, P.; Marsella, A. Oxychlorination of Ethylene in Two Stage Fixed-bed Reactor. US Patent, US5841009A, 1998.
(87) Schussler, H. W., III Oxychlorination Catalyst. US Patent, US6174834, 2001.
(88) Marsella, A.; Fatutto, P.; Carmello, D. Catalyst and Oxychlorination Process Using It. US Patent, US6465701, 2002.
(89) Marsella, A.; Vidotto, S.; Cremaschi, B. Hollow Pellet Suitable as Carrier of Catalysts for Selective Exothermic Reactions. US Patent, US7141708B2, 2006.
(90) Strebelle, M.; Petitjean, A. Oxychlorination Catalyst and Process Using Such a Catalyst. US Patent, US7807604B2, 2010.
(91) Orsenigo, C.; Casagrande, F.; Civati, M. Catalysts for Fixed Bed Oxychlorination of Ethylene to 1.2-Dichloroethane. US Patent, US8216960B2, 2012.

https://dx.doi.org/10.1021/acscatal.0c01698
ACS Catal. 2020, 10, 9299−9319

(92) Zurowski, K. DTA analysis of the System Carrier-$CuCl_2$, KCl. *J. Therm. Anal.* **1990**, *36*, 947−955.
(93) de Miguel, S. R.; Scelza, O. A.; Castro, A. A.; Soria, J. Characterization of γ-alumina Doped with Li and K by Infrared Studies of CO Adsorption and 27 Al-NMR. *Top. Catal.* **1994**, *1*, 87−94.
(94) Żurowski, K. Some Aspects of the Phase Changes of the $CuCl_2$− KCl System. *J. Therm. Anal.* **1995**, *44*, 197−204.
(95) Liu, J.; Xueju, L.; Zhou, G.; Zhen, K.; Zhang, W.; Cheng, T. Effect of KCl on $CuCl_2/\gamma$-Al_2O_3 Catalyst for Oxychlorination of Ethane. *React. Kinet. Catal. Lett.* **2006**, *88*, 315−324.
(96) Kosaka, Y.; Hayata, M.; Toyo Soda Co, Y. J. Oxychlorination of Hydrocarbons. I. Synthesis of 1,2-Dichloroethane by Oxychlorination of Ethylene Using a $NaHSO_4NH_4HSO_4$-$CuCl_2$ catalyst. *Kogyo Kagaku Zassh* **1966**, *69*, 244−248.
(97) García, C. L.; Resasco, D. E. Promoter Action of KCl on $CuCl_2/SiO_2$ Catalysts Used for the Oxyhydrochlorination of Methane. *Appl. Catal.* **1987**, *29*, 55−66.
(98) Zurowski, K. The Mechanism of the Ethene Oxychlorination Process when $CuCl_2$,KCl-Support Catalyst is Used. *Polym. J. Chem.* **1995**, *69*, 1718−1728.
(99) Repelewicz, M. Activity of Cupric Chloride-Potassium Chloride-Carrier Catalysts in Oxidation and Oxychlorination of Ethylene. *Polym. J. Appl. Chem.* **1992**, *36*, 177−182.
(100) Prasad, P. S. S.; Rao, P. K. Low-temperature Ethylene Chemisorption (LTEC)-a Novel Technique for the Characterization of $CuCl_2$-KCl gamma-Al_2O_3 Oxychlorination Catalysts. *J. Chem. Soc., Chem. Commun.* **1987**, 951−953.
(101) Carmello, D.; Garilli, M.; Fatutto, P.; Caccialupi, L. Catalyst, Process for Its Preparation, and Its Use in the Synthesis of 1,2-Dichloroethane. US Patent, US6777373B1, 2004.
(102) Orsenigo, C.; Casagrande, F.; Civati, M. Catalysts for Fixed Bed Oxychlorination of Ethylene to 1.2-Dichloroethane. US Patent, US8216960B2, 2010.
(103) Xueju, L.; Jie, L.; Guangdong, Z.; Kaiji, Z.; Wenxing, L.; Tiexin, C. Ethane Oxychlorination' over gamma-Al_2O_3 Supported $CuCl_2$-CoKCl-$CoLaCl_3$. *Catal. Lett.* **2005**, *100*, 153−159.
(104) Little, J. A.; Kenney, C. N. A Microstructural Study of a Supported Liquid Phase Oxychlorination Catalyst. *J. Catal.* **1985**, *93*, 23−29.
(105) Villadsen, J.; Livejerg, H. Supportsd Liquid-Phass Catalysts. *Catal. Rev.: Sci. Eng.* **1978**, *17*, 203−272.
(106) Li, C.; Zhou, G.; Wang, L.; Dong, S.; Li, J.; Cheng, T. Effect of Ceria on the MgO-γ-Al_2O_3 Supported $CeO_2/CuCl_2$/KCl Catalysts for Ethane Oxychlorination. *Appl. Catal., A* **2011**, *400*, 104−110.
(107) Cavalli, L.; Rubini, C. Catalysts for the Oxychlorination of Ethylene, Method for Preparing Them, and Oxichlorination Method Using the Same. US Patent, US5905054A, 1999.
(108) Eden, J. S. Copper Catalyst Compositions for Fluid-bed Oxyhydrochlorination of Ethylene. US Patent, US4446249A, 1984.
(109) Derleth, H.; Adem, D.; Strebelle, M. Catalytic Compositon and Process for the Oxychlorination of Ethylene Using Such a Composition. US Patent, US6803342B1, 2004.
(110) Eichhorn, H. D.; Mross, W. D.; Schachner, H.; Schwarzmann, M. Molded Supported Catalyst. US Patent, US4753914A, 1988.
(111) Ma, H.; Fenes, E.; Qi, Y.; Wang, Y.; Rout, K. R.; Fuglerud, T.; Chen, D. Understanding of K and Mg Co-promoter Effect in Ethylene Oxychlorination by Operando UV-vis-NIR Spectroscopy. *Catal. Today* **2020**, DOI: 10.1016/j.cattod.2020.06.049.
(112) Kuhrs, C.; Meissner, R. Catalyst Composition for Oxychlorination. US Patent, US7126035B2, 2006.
(113) Heinemann, H.; Spector, M. L.; Wender, L.; Yarze, J. C.; Kellogg Co, M. W.; P. N, J. U. S. A. Oxychlorination of Ethylene by Homogeneous Catalysis. *Erdoel Kohle* **1967**, *20*, 400−404.
(114) Flid, M. R. Problems of Increase in the Selectivity of Ethylene Oxychlorination Processes: II. General Patterns in the Formation of Chloroorganic Byproducts in the Ethylene Oxychlorination Process. *Catal. Ind.* **2016**, *8*, 23−31.
(115) Flid, M. R. Problems of Increase in the Selectivity of Ethylene Oxychlorination Processes: I. General Patterns in the Formation of Carbon Oxides in the Ethylene Oxychlorination Process. *Catal. Ind.* **2015**, *7*, 119−127.
(116) Jaqueau, D.; Piester, L. W.; Bohl, L. E.; Knoop, J. F. Oxychlorination. *Chem. Ing. Tech.* **1971**, *43*, 184−187.
(117) Lester, G. R. Catalytic Destruction of Hazardous Halogenated Organic Chemicals. *Catal. Today* **1999**, *53*, 407−418.
(118) Mile, B.; Ryan, T.; Tribbeck, T.; Zammitt, M.; Hughes, G. Kinetic Studies of the Dehydrochlorination of 1, 2-Dichloroethane on Alumina Supported Copper (II) Chloride Catalysts. *Top. Catal.* **1994**, *1*, 153−162.
(119) Feijen-Jeurissen, M. M. R.; Jorna, J. J.; Nieuwenhuys, B. E.; Sinquin, G.; Petit, C.; Hindermann, J.-P. Mechanism of Catalytic Destruction of 1,2-Dichloroethane and Trichloroethylene over γ-Al_2O_3 and γ-Al_2O_3 Supported Chromium and Palladium Catalysts. *Catal. Today* **1999**, *54*, 65−79.
(120) Avdeev, V. I.; Kovalchuk, V. I.; Zhidomirov, G. M.; d'Itri, J. L. Models of Active Sites in Supported Cu Metal Catalysts In 1,2-Dichloroethane Dechlorination. DFT analysis. *J. Struct. Chem.* **2007**, *48*, S160−S170.
(121) Carmello, D.; Finocchio, E.; Marsella, A.; Cremaschi, B.; Leofanti, G.; Padovan, M.; Busca, G. An FT-IR and Reactor Study of the Dehydrochlorination Activity of $CuCl_2$/gamma-Al_2O_3-based Oxychlorination Catalysts. *J. Catal.* **2000**, *191*, 354−363.
(122) Shalygin, A. S.; Malysheva, L. V.; Paukshtis, E. A. Mechanism of 1,2-Dichloroethane Dehydrochlorination on the Acid Sites of Oxide Catalysts as Studied by IR Spectroscopy. *Kinet. Catal.* **2011**, *52*, 305−315.
(123) Gel'perin, E. I.; Bakshi, Yu. M.; Zyskin, A. G.; Snagovskii, Yu.S.; Avetisov, A. K. *Khim. Prom-st.* **1996**, *6*, 356.
(124) Derouane, E.; Parmon, V.; Lemos, F.; Ribeiro, F. *Principles and Methods for Accelerated Catalyst Design and Testing*: Springer Science and Business Media: 2002; DOI: 10.1007/978-94-010-0554-8.
(125) Naumburg, K.; Schwedler, G.; Emig, G. Kinetische Untersuchungen Zur Katalytischen Gasphasenchlorierung Von Äthylen Mit Sauerstoff Und Wäßriger Salzsäure. *Chem. Ing. Tech.* **1967**, *39*, 505−510.
(126) Eichhorn, H. D.; Jackh, C.; Mross, W. D.; Schuler, H. Activity and Selectivity Relationships in the Oxychlorination of Ethylene on $CuCl_2$-KCl/γ-Al_2O_3 Catalysts. 8th Int. Congress on Catalysis, 1984; p 647.
(127) Zhong, B.; Zhao, J. Kinetics of Oxychlorination of Ethylene over Copper Catalysts. *Shiyou Huagong* **1985**, *4*, 23−28.
(128) Chen, F.; Yang, Y.; Rong, S.; Chen, G. Studies on Ethylene Oxychlorination II. Reaction Mechanism and Kinetics. *Shiyou Huagong* **1994**, *7*, 421−425.
(129) Bakshi, Y. M.; Gelbshtein, A. I.; Gelperin, E. I.; Dmitrieva, M. P.; Zyskin, A. G.; Snagovskii, Y. S. Study of the Mechanism and Kinetics of Additive Oxychlorination of Olefins 0.5. Kinetic-Model of the Reaction. *Kinet. Catal.* **1991**, *32*, 663−672.
(130) Wachi, S.; Asai, Y. Kinetics of 1,2-Dichloroethane Formation from Ethylene and Cupric Chloride. *Ind. Eng. Chem. Res.* **1994**, *33*, 259−264.
(131) Montebelli, A.; Tronconi, E.; Orsenigo, C.; Ballarini, N. Kinetic and Modeling Study of the Ethylene Oxychlorination to 1,2-Dichloroethane in Fluidized-bed Reactors. *Ind. Eng. Chem. Res.* **2015**, *54*, 9513−9524.

https://dx.doi.org/10.1021/acscatal.0c01698
ACS Catal. 2020, 10, 9299−9319